

Electronic Supplementary Information

for

A supramolecular photocatalyst composed of a polyoxometalate and a photosensitizing water-soluble porphyrin diacid for oxidation of organic substrates in water

Tomoya Ishizuka,^a Shumpei Ohkawa,^a Hidemi Ochiai,^a Muneaki Hashimoto,^a Kei Ohkubo,^{b, c} Hiroaki Kotani,^a Masahiro Sadakane,^d Shunichi Fukuzumi^{c, e} and Takahiko Kojima*^a

^a *Department of Chemistry, Graduate School of Pure and Applied Sciences, University of Tsukuba, 1-1-1 Tennoudai, Tsukuba, Ibaraki 305-8571, Japan.*

^b *Institute for Advanced Co-Creation Studies and Institute for Academic Initiatives, Osaka University, Suita, Osaka 565-0871, Japan*

^c *Department of Chemistry and Nano Science, Ewha Womans University, Seoul 120-750, Korea.*

^d *Department of Applied Chemistry, Graduate School of Engineering, Hiroshima University, 1-4-1 Kagamiyama, Higashi Hiroshima 739-8527, Japan.*

^e *Faculty of Science and Technology, Meijo University, Tempaku, Nagoya, Aichi 468-8502, Japan.*

General.

Chemicals and solvents were purchased from commercial sources and used as received unless otherwise mentioned. All reactions were performed under an Ar atmosphere unless otherwise stated. MeCN was distilled over CaH₂ under Ar before use. Diethyl ether, THF, toluene and 1,4-dioxane were distilled over Na/benzophenone under Ar before use. *N,N*-dimethylacetamide (DMA) and *N,N*-dimethylformamide (DMF) were distilled over MgSO₄ under Ar before use. Tetrakis(*N*-methyl-pyrid-4-yl)porphyrin was purchased from Aldrich. Keggin-type polyoxometalates, K₅H[CoW₁₂O₄₀],¹ K₆[GeW₁₁O₃₉Mn(H₂O)],² K₄[PW₁₁O₃₉-Mn(H₂O)],^{2,3} K₅[PW₁₁O₃₉Mn(H₂O)],² K₆[SiW₁₁O₃₉Mn(H₂O)],² K₅[SiW₁₁O₃₉-Ru(H₂O)] (RuPOM),⁴ and a Dawson-type polyoxometalate, K₇[P₂W₁₇O₆₁Mn(H₂O)],³ were prepared in accordance with literature methods.

¹H NMR measurements were performed on JEOL JNM-ECS400 and Bruker AVANCE-400 and DPX-400 spectrometers. MALDI-TOF-MS spectra were measured on Bruker UltrafleXtreme-TN MALDI-TOF/TOF and AB SCIEX TOF/TOF 5800 spectrometers by using dithranol and 9-nitroanthracene as a matrix. ESI-TOF-MS spectra were measured on a JEOL JMS-T100CS spectrometer. UV-Vis absorption spectra were measured on a SHIMADZU UV-2450 spectrophotometer at room temperature. Emission spectra were measured on a HORIBA Scientific FluoroMax-4 spectrometer. IR spectra were measured on a JASCO FT/IR-550 spectrometer using KBr disks in the range of 400 – 4000 cm⁻¹. Elemental analyses were performed at Department of Chemistry, University of Tsukuba.

Synthesis.

Route 1 (Scheme S1):

α -Azidostyrene. α -Azidostyrene was synthesized according to the literature method.⁵ NaN₃ (2.04 g, 31.4 mmol) was dissolved in MeCN (60 mL) with stirring at 0 °C for 25 min in the dark. ICl (*ca.* 1.7 mL, 35 mmol) in MeCN (60 mL) was added dropwise to the NaN₃ solution, and stirred at 0 °C for 1.5 h in the dark. A solution of styrene (3.5 mL, 30 mmol) in MeCN (10 mL) was added dropwise to the reaction mixture, and stirred at 0 °C for 15 h in the dark. After addition of water to the reaction mixture, the mixture was extracted with Et₂O and the organic phase was dried over Na₂SO₄. The organic phase was concentrated with a rotary evaporator, and during the concentration,

the organic phase was separated into two phases. The lower phase was separated and diluted with Et₂O (80 mL) and KO^t-Bu (5.01 g, 44.6 mmol) was added to the solution. The reaction mixture was stirred at room temperature for 5 h in the dark. After addition of water, the reaction mixture was extracted with AcOEt, washed with brine, and the organic phase was dried over Na₂SO₄. The organic phase was concentrated and hexane was added to it. The precipitate was filtered off and the solvent of the filtrate was evaporated to dryness at 30 °C. The residual oil was purified with column chromatography on silica gel by using hexane as an eluent. The fraction was collected and evaporation of the solvent of the fraction at 30 °C gave a pale yellow oil of α -azidostyrene (2.81 g, 19.4 mmol, 64%). ¹H NMR (CDCl₃): δ 4.97 (d, J = 2.4 Hz, 1H, =CH₂ at the *cis*-position of the N₃ group), 5.44 (d, J = 2.4 Hz, 1H, =CH₂ at the *trans*-position of the N₃ group), 7.36 – 7.58 (m, 5H, phenyl-H).

3,4-Diphenylpyrrole. 3,4-Diphenylpyrrole was synthesized according to the literature method.⁶ NiCl₂ (86.1mg, 0.66 mmol), α -azidostyrene (2.62 g, 18.0 mmol) and phenylacetaldehyde (2.01 mL, 18.0 mmol) were dissolved in DMA and the reaction mixture was stirred at 110 °C for 4 h in the dark. After addition of water, the reaction mixture was extracted with AcOEt, washed with brine, and the organic phase was dried over Na₂SO₄. The solvent of the organic phase was evaporated and the residual oil was purified with column chromatography on silica gel by using hexane/AcOEt (8 : 1, v/v) as an eluent. The fraction was collected and evaporation of the solvent of the fraction gave a dark brown oil of 3,4-diphenylpyrrole (2.51 g, 11.4 mmol, 64%). ¹H NMR (CDCl₃): δ 6.93 (d, J = 2.8 Hz, 2H, pyrrole- α -H), 7.15 – 7.29 (m, 10H, phenyl-H), 8.32 (br s, 1H, pyrrole-NH).

Diprotonated 2,3,7,8,12,13,17,18-octaphenyl-5,10,15,20-tetrakis-(*p*-bromophenyl)-porphyrin (H₄2²⁺). H₄2²⁺ was synthesized according to the literature method.⁷ 3,4-Diphenylpyrrole (1.70 g, 7.73 mmol), *p*-bromobenzaldehyde (1.45 g, 7.82 mmol) and NaCl (59.4 mg, 1.02 mmol) were combined in CH₂Cl₂ (850 mL) with stirring at room temperature for 10 min in the dark. BF₃·OEt₂ (0.37 mL, 2.9 mmol) was added to the reaction mixture and the reaction mixture was stirred at room temperature for 28 h in the dark. After removal of the solvent of the reaction mixture under vacuum, the residual solid was dissolved in toluene (450 mL) and 2,3-dichloro-5,6-dicyano-1,4-benzoquinone (DDQ; 1.77 g, 3.76 mmol) and triethylamine (0.85 mL, 6.1 mmol) were added to the solution. The reaction mixture was refluxed for 40 h in the dark under

air. The mixture was concentrated to a small volume and passed through an alumina column with use of CH_2Cl_2 as an eluent. The solvent of the collected fraction was evaporated to dryness. The residue was purified with column chromatography on silica gel using $\text{CH}_2\text{Cl}_2/\text{MeOH}$ (99 : 1, v/v) as an eluent. The solvent of the collected fraction was evaporated and the residue was recrystallized from the CHCl_3 solution in the presence of 12 M HCl (3 drops) and hexane as a poor solvent to give dark green crystals of $[\text{H}_4\text{2}^{2+}]\text{Cl}_2$ (299 mg, 0.19 mmol, 9.6%). ^1H NMR (CDCl_3): δ 6.72 – 6.85 (m, 40H, β -phenyl-H), 7.18 (d, $J = 8.4$ Hz, 8H, *meso*-phenyl-*m*-H), 7.72 (d, $J = 8.4$ Hz, 8H, *meso*-phenyl-*o*-H). UV-Vis (CHCl_3): λ_{max} [nm] = 489, 702. MS (MALDI-TOF, dithranol matrix): $m/z = 1539.5$ (calcd. for $[\text{M} - \text{H}]^+$: 1539.2).

2,3,7,8,12,13,17,18-Octaphenyl-5,10,15,20-tetrakis(pyrid-4-yl-phenyl)porphyrin

(H₂3). Porphyrin $\text{H}_4\text{2}^{2+}$ (88.7 mg, 51.8 μmol), 4-(4,4,5,5-tetramethyl-1,3,2-dioxaborolan-2-yl)pyridine (118 mg, 0.58 mmol), K_2CO_3 (305 mg, 2.21 mmol) and $\text{Pd}(\text{PPh}_3)_4$ (88.2 mg, 76.3 μmol) were combined in a mixed solvent of 1,4-dioxane (8.8 mL) and H_2O (1.8 mL). After the reaction mixture was degassed with freeze-pump-thaw cycles (3 times), it was refluxed for 36 h in the dark. The reaction mixture was evaporated to dryness and the residue obtained was purified with column chromatography on silica gel using a mixed solvent of $\text{CH}_2\text{Cl}_2/\text{MeOH}/\text{Et}_3\text{N}$ (94.5 : 5 : 0.5, v/v/v) as an eluent. The collected fraction was evaporated to dryness and the residue was recrystallized from $\text{CHCl}_3/\text{hexane}$ to give dark green crystals of **H₂3** (52.7 mg, 37.3 μmol , 72%). ^1H NMR (CD_3OD): δ 6.54 – 6.91 (m, 40H, β -phenyl-H), 7.33 (br s, 8H, *meso*-phenyl-*o*-H), 7.61 (d, $J = 6.0$ Hz, 8H, pyridyl-*m*-H), 7.99 (br s, 8H, *meso*-phenyl-*m*-H), 8.65 (d, $J = 6.0$ Hz, 8H, pyridyl-*o*-H). UV-Vis (MeOH): λ_{max} [nm] = 485, 721. MS (MALDI-TOF, dithranol matrix): $m/z = 1534.3$ (calcd. for $[\text{M} + 2\text{H}]^+$: 1533.8).

Diprotonated 2,3,7,8,12,13,17,18-octaphenyl-5,10,15,20-tetrakis(*N*-methylpyridinium-4-yl)-phenyl-porphyrin hexachloride salt ($[\text{H}_4\text{1}^{6+}]\text{Cl}_6$). **H₂3** (21.2 mg, 13.8 μmol) and $\text{Cu}(\text{OAc})_2 \cdot \text{H}_2\text{O}$ (7.67 mg, 38.4 μmol) were dissolved in DMF (6.0 mL) and stirred at 40 °C for 3 h in the dark. After the reaction mixture was evaporated to dryness, the residue was dissolved in CH_2Cl_2 and washed with brine. The solvent was removed under reduced pressure and dried under vacuum for 2 h. DMF (1.7 mL), K_2CO_3 (43.3 mg, 0.31 mmol) and MeI (0.18 mL, 27.3 mmol) were added to the residue and the mixture was stirred at 40 °C for 4 days in the dark. Then, H_2O and excess

amount of NH_4PF_6 were added to the reaction mixture to give dark green precipitate, which was separated by filtration. The precipitate was dissolved in MeOH (5.7 mL) containing *conc.* HCl (0.58 mL, 5.73 mmol), and the reaction mixture was stirred at room temperature for 24 h in the dark. Then, excess amount of NH_4PF_6 and H_2O was added to the reaction mixture to obtain red-brown precipitate. The precipitate was purified with column chromatography on silica gel by using a mixed solvent of MeCN : $\text{H}_2\text{O} = 9 : 1$ (v/v) saturated with KNO_3 as an eluent. The solvent of the collected fraction was evaporated and the residue was recrystallized from MeOH/AcOEt. The counter anion of the obtained dark brown solid was exchanged with ion-exchange column by using the mixed solvent of 0.1 M NaCl aq and 3 M HCl aq/MeOH (2 : 1, v/v) as an eluent. The fraction was neutralized with NaHCO_3 and the volatile was evaporated. The residue was purified by size-exclusion chromatography on Sephadex LH-20 with MeOH as an eluent. The solvent of the collected fraction was evaporated and the residue was recrystallized from MeOH in the presence of 1 drop of *conc.* HCl and AcOEt as a poor solvent to give brown crystals of $[\text{H}_4\mathbf{1}^{6+}]\text{Cl}_6$ (9.43 mg, 5.22 μmol , 38%). The characterization data of $[\text{H}_4\mathbf{1}^{6+}]\text{Cl}_6$ are shown in the paragraph for another procedure of $[\text{H}_4\mathbf{1}^{6+}]\text{Cl}_6$ in Route 2.

Route 2 (Scheme S2):

2-(4-Bromophenyl)-1,3-dioxane. 2-(4-Bromophenyl)-1,3-dioxane was synthesized according to the literature method.⁸ 4-Bromobenzaldehyde (3.02 mg, 16.3 mmol) and 1,3-propanediol (1.9 mL, 26 mmol) were dissolved in toluene (40 mL) and the reaction mixture was refluxed for 4 h. $\text{BF}_3 \cdot \text{OEt}_2$ (0.50 mL, 7.89 mmol) was added to the reaction mixture and the reaction mixture was refluxed for 1 h. The reaction mixture was cooled to room temperature and washed by 1 M NaHCO_3 aq, H_2O and brine. The organic phase was dried over MgSO_4 and evaporated to give white crystals of 2-(4-bromophenyl)-1,3-dioxane (3.39 g, 14.0 mmol, 86%). ^1H NMR (CDCl_3): δ 1.45 (d, $J = 13.6$ Hz, 1H, dioxane-H5), 2.21 (m, 1H, dioxane-H5), 3.98 (td, $J = 12.4, 2.4$ Hz, 2H, dioxane-H4, H6), 4.26 (dd, $J = 11.2, 4.8$ Hz, 2H, dioxane-H4, H6), 5.46 (s, 1H, dioxane-H2), 7.36 (d, $J = 8.4$ Hz, 2H, phenyl-*o*-H), 7.49 (d, $J = 8.4$ Hz, 2H, phenyl-*m*-H).

4-Formyl-phenylboronic acid. To 2-(4-bromophenyl)-1,3-dioxane (3.51 g, 14.4 mmol) in THF (15 mL) was added Mg (1.36 g, 60.0 mmol) and 5 drops of 1,2-dibromoethane and stirred for 10 min. Subsequently, a solution of 2-(4-bromophenyl)-1,3-dioxane (7.01 g, 28.9 mmol) in THF (30 mL) was further added dropwise to the mixture and the

mixture was stirred for 1.5 h. Trimethylborate (5.0 mL, 44.8 mmol) was added to the mixture and the reaction mixture was stirred for 40 min. Residual Mg was quenched by addition of *conc.* HCl aq with stirring for further 30 min. After filtration of the reaction mixture, the filtrate was extracted with AcOEt. The organic phase was dried over Na₂SO₄ and the solvent was evaporated to dryness. H₂O (60 mL) and *conc.* HCl aq (20 mL) were added to the residue and the mixture was refluxed for 1 h. The hot mixture was filtered and the filtrate was cooled to room temperature. Precipitate formed was filtered to give yellow powder of 4-formyl-phenyl-boronic acid (2.88 g, 21.0 mmol, 48%). ¹H NMR (acetone-*d*₆): δ 7.46 (s, 2H, OH), 7.90 (d, *J* = 8.0 Hz, 2H, phenyl-*o*-H), 8.06 (d, *J* = 8.0 Hz, 8H, phenyl-*m*-H), 10.08 (s, 1H, CHO).

4-Pyrid-4'-yl-benzaldehyde. 4-Pyrid-4'-yl-benzaldehyde was synthesized according to the literature method.⁹ 4-formyl-phenyl-boronic acid (1.15 g, 7.69 mmol), 4-bromopyridine hydrochloride (1.01 g, 5.19 mmol), KCO₃ (2.84 g, 20.5 mmol) and Pd(PPh₃)₄ (287 mg, 0.25 mmol) were dissolved in a mixed solvent of 1,4-dioxane (20 mL) and H₂O (5 mL). After the reaction mixture was degassed with freeze-pump-thaw cycles (4 times), it was refluxed for 13 h in the dark. The reaction mixture was extracted with CH₂Cl₂ and the organic phase was dried over MgSO₄. After removal of the solvent, the residue was purified with column chromatography on silica gel by using AcOEt/hexane (3 : 1, v/v) as an eluent. The fraction was collected and evaporation of the solvent of the fraction gave a beige powder of 4-pyrid-4'-yl-benzaldehyde (796 mg, 5.34 mmol, 84%). ¹H NMR (CDCl₃): δ 7.54 (d, *J* = 6.0 Hz, 2H, pyridyl-*m*-H), 7.80 (d, *J* = 8.4 Hz, 2H, phenyl-*m*-H), 8.01 (d, *J* = 8.0 Hz, 2H, phenyl-*o*-H), 8.73 (d, *J* = 6.0 Hz, 2H, pyridyl-*o*-H), 10.10 (s, 1H, CHO).

4-(4'-Formylphenyl)-*N*-methyl-pyridinium hexafluorophosphate. 4-Pyrid-4'-yl-benzaldehyde (0.979 g, 5.34 mmol) was dissolved in MeCN (30 mL) and MeI (3.0 mL, 48.2 mmol) was added to the mixture. The mixture was refluxed for 15 h and excess NH₄PF₆ aq was added to the mixture. Filtration of the precipitate gave yellow powder of 4-(4'-formylphenyl)-*N*-methyl-4-pyridinium hexafluorophosphate (1.55 g, 4.52 mmol, 84%). ¹H NMR (CD₃CN): δ 4.30 (s, 3 H, CH₃), 8.07 (d, *J* = 8.8 Hz, 2H, phenyl-*o*-H), 8.12 (d, *J* = 8.8 Hz, 2H, phenyl-*m*-H), 8.28 (d, *J* = 6.8 Hz, 2H, pyridyl-*m*-H), 8.67 (d, *J* = 6.8 Hz, 2H, pyridyl-*o*-H), 10.12 (s, 1H, CHO).

Diprotonated 2,3,7,8,12,13,17,18-octaphenyl-5,10,15,20-tetrakis[*N*-methylpyridinium-4-yl]-phenyl]-porphyrin hexachloride salt ([H₄1⁶⁺]Cl₆).

4-(4'-Formylphenyl)-*N*-methyl-4-pyridinium hexafluorophosphate (900 mg, 2.62 mmol) and 1,3-diphenylpyrrole (576 mg, 2.63 mmol) were dissolved in CH₂Cl₂ (260 mL) and stirred for 20 min. BF₃·etherate (99 μL, 0.79 mmol) was added to the mixture and stirred for 22 h in the dark. After evaporation of the solvent of the reaction mixture, MeCN (92 mL) and DDQ (418 mg, 1.84 mmol) and triethylamine (80 μL, 0.58 mmol) were added to the residue and the mixture was refluxed for 21 h in the dark. The solvent of the mixture was evaporated to dryness, and the residue was purified with column chromatography on silica gel using a mixed solvent (MeCN : H₂O = 9 : 1 (v/v)) saturated with KNO₃ as an eluent. The solvent of the collected fraction was evaporated and residual solids obtained were washed with H₂O to remove inorganic salts. The residual solid and an anion-exchange resin (Cl⁻ form, DOWEXTM MARATHONTM A2 Resin) were suspended in H₂O and stirred for 16 h. After removal of resin by filtration, the solvent of the filtrate was evaporated. The residue was recrystallized from MeOH in the presence of 1 drop of *conc.* HCl aq and 1,2-dimethoxyethane as a poor solvent to give green crystals of [H₄1⁶⁺]Cl₆ (97.2 mg, 53.8 μmol, 8%). ¹H NMR (CD₃CN): δ 4.40 (s, 12H, CH₃), 6.78 (br s, 40H, β-phenyl), 7.65 (d, *J* = 8.4 Hz, 8H, phenyl-*m*-H), 8.18 (d, *J* = 6.8 Hz, 8H, pyridyl-*m*-H), 8.44 (d, *J* = 8.4 Hz, 8H, phenyl-*o*-H), 8.82 (d, *J* = 6.8 Hz, 8H, pyridyl-*o*-H). ESI-TOF-MS (MeOH): *m/z* = 530.19 (calcd. for [H1]³⁺: 530.24). Anal. calcd. for C₁₁₆H₈₈N₈Cl₆ · 18H₂O: C 64.97, H 5.97, N 5.12; Found: C 65.03, H 5.85, N 5.12.

Infrared Spectroscopy and MALDI-TOF MS Spectrometry for the Supramolecular Assemblies of H₄1⁶⁺ with POMs.

The supramolecular assemblies analysed by FT-IR spectroscopy and MALDI-TOF MS spectrometry were obtained as follows: To an aqueous solution of H₄1²⁺ (1.0 mM) was added 0.5 equiv of one of the POMs, and the resultant suspension was centrifuged to be separated into precipitate and filtrate. After removing the filtrate, the obtained precipitate was dried under vacuum. FT-IR spectra were measured with a JASCO FT/IR spectrometer with KBr pellet samples, fabricated with the precipitated solid samples of the supramolecular assemblies, at room temperature. The characteristic vibration bands are summarized in Table S2. MALDI-TOF MS spectrometry of the supramolecular assemblies was performed on an AB SCIEX TOF/TOF 5800 spectrometer with the linear mode, using dithranol as a matrix.

$\{(\mathbf{H}_4\mathbf{1})_2[\mathbf{CoW}_{12}\mathbf{O}_{40}]\}^{6+}$: ν [cm^{-1}] = 3051, 1635, 1525, 1471, 1339, 1295, 1201, 932, 869, 759. m/z = 3091.07 (calcd for $[\{(\mathbf{H}_2\mathbf{1})_2(\mathbf{CoW}_{12}\mathbf{O}_{40})\} + 6\text{Cl} - 8\text{CH}_3]^{2+}$: 3091.714).

$\{(\mathbf{H}_4\mathbf{1})_2[\mathbf{GeW}_{11}\mathbf{O}_{39}\mathbf{Mn}(\mathbf{H}_2\mathbf{O})]\}^{6+}$: ν [cm^{-1}] = 3047, 1636, 1473, 1407, 1294, 1201, 945, 879, 810, 703. m/z = 3085.59 (calcd for $[\{(\mathbf{H}_4\mathbf{1})_2(\mathbf{GeW}_{11}\mathbf{O}_{39}\mathbf{Mn}(\mathbf{H}_2\mathbf{O}))\} + 7\text{Cl} - 4\text{CH}_3]^{2+}$: 3084.922).

$\{(\mathbf{H}_4\mathbf{1})_2[\mathbf{P}_2\mathbf{W}_{17}\mathbf{O}_{61}\mathbf{Mn}(\mathbf{H}_2\mathbf{O})]\}^{5+}$: ν [cm^{-1}] = 3047, 1634, 1525, 1472, 1405, 1083, 946, 912. m/z = 3088.48 (calcd for $[\{(\mathbf{H}_4\mathbf{1})(\mathbf{P}_2\mathbf{W}_{17}\mathbf{O}_{61}\mathbf{Mn}(\mathbf{H}_2\mathbf{O}))\} + 11\text{Cl} + 2\text{H} - 3\text{CH}_3]^{2+}$: 3088.53).

$\{(\mathbf{H}_4\mathbf{1})_2[\mathbf{PW}_{11}\mathbf{O}_{39}\mathbf{Mn}(\mathbf{H}_2\mathbf{O})]\}^{8+}$: ν [cm^{-1}] = 3047, 1636, 1295, 1193, 1074, 961, 881. m/z = 3151.29 (calcd for $[\{(\mathbf{H}_4\mathbf{1})_2(\mathbf{PW}_{11}\mathbf{O}_{39}\mathbf{Mn}(\mathbf{H}_2\mathbf{O}))\} + 11\text{Cl} + 2\text{H} - 2\text{CH}_3]^{2+}$: 3151.050).

$\{(\mathbf{H}_4\mathbf{1})_2[\mathbf{PW}_{11}\mathbf{O}_{39}\mathbf{Mn}(\mathbf{H}_2\mathbf{O})]\}^{7+}$: ν [cm^{-1}] = 3042, 1636, 1525, 1441, 1200, 1075, 1048, 949, 809. m/z = 3086.53 (calcd for $[\{(\mathbf{H}_4\mathbf{1})_2(\mathbf{PW}_{11}\mathbf{O}_{39}\mathbf{Mn}(\mathbf{H}_2\mathbf{O}))\} + 7\text{Cl} - \text{CH}_3]^{2+}$: 3086.654).

$\{(\mathbf{H}_4\mathbf{1})_2[\mathbf{SiW}_{11}\mathbf{O}_{39}\mathbf{Mn}(\mathbf{H}_2\mathbf{O})]\}^{6+}$: ν [cm^{-1}] = 3037, 1635, 1472, 1404, 1210, 1012, 993, 948, 903. m/z = 3070.38 (calcd for $[\{(\mathbf{H}_4\mathbf{1})_2(\mathbf{SiW}_{11}\mathbf{O}_{39}\mathbf{Mn}(\mathbf{H}_2\mathbf{O}))\} + 6\text{Cl} - 8\text{H}]^{2+}$: 3070.97).

$\{(\mathbf{H}_4\mathbf{1})_2[\mathbf{RuPOM}]\}^{7+}$: ν [cm^{-1}] = 3053, 1636, 1527, 1471, 1405, 1296, 956, 910, 785. m/z = 3091.84 (calcd for $[\{(\mathbf{H}_2\mathbf{1})_2(\mathbf{SiW}_{11}\mathbf{O}_{39}\mathbf{Ru}(\mathbf{H}_2\mathbf{O}))\} + 7\text{Cl} - 3\text{CH}_3]^{2+}$: 3091.223).

X-ray Crystallography.

Single crystals of $[\mathbf{H}_4\mathbf{1}^{6+}]\text{Cl}_6$ suitable for X-ray crystallography were obtained by recrystallization with a vapour-diffusion method to the MeOH solution with 1,2-dimethoxyethane as a poor solvent. A crystal was mounted on a mounting loop. All diffraction data were collected on a Bruker APEXII diffractometer at 120 K with graphite monochromated Mo $K\alpha$ ($\lambda = 0.71073 \text{ \AA}$) by the 2θ - ω scan. The structure was solved by a direct method using SIR97 and SHELX97.¹⁰ Co-crystallized MeOH and DME molecules were severely disordered and thus their contribution was subtracted from the diffraction pattern by the “Squeeze” program.¹¹ Crystallographic data for $[\mathbf{H}_4\mathbf{1}^{6+}]\text{Cl}_6$ are summarized in Table S5. CCDC-1549180 contains supplementary crystallographic data for $[\mathbf{H}_4\mathbf{1}^{6+}]\text{Cl}_6$.

Electrochemical Studies.

Cyclic and differential-pulse voltammograms of $\text{H}_4\mathbf{1}^{6+}$ (0.7 mM) were recorded in CH_3CN , containing TBAPF_6 (0.1 M) as an electrolyte, at 298 K under Ar, on a BAS electrochemical analyser Model 660A (Figure S5). Differential-pulse voltammograms of $\text{H}_4\mathbf{1}^{6+}$ (0.1 mM) were also measured at 298 K under Ar in hexamine buffer containing NaCl (0.1 M) as an electrolyte, whose pH was varied with addition of NaOH aq (15 M).

Determination of $\text{p}K_a$.

Determination of the $\text{p}K_a$ values of $\text{H}_4\mathbf{1}^{6+}$ was carried out by spectroscopic pH titration experiments and curve fitting on the basis of the equation (1). The titration was

$$A_{\text{obs}} = A_0 + \frac{A_{\infty} - A_0}{K_a \times 10^{-\text{pH}} + 1} \quad (\text{S1})$$

done as follows; to the solution of $\text{H}_2\mathbf{1}^{6+}$ in hexamine buffer at pH 2.71, aliquots of NaOH (15 M) were added to increase the pH value and the absorption change was monitored at 632 nm for $\text{p}K_{a2}$ and at 518 nm for $\text{p}K_{a1}$.

Determination of the Association Ratio of $\text{H}_4\mathbf{1}^{6+}$ with POMs by Job's Plot.

Job's analysis for the association of $\text{H}_4\mathbf{1}^{6+}$ with POMs was carried out using solutions containing $\text{H}_4\mathbf{1}^{6+} + \text{RuPOM}$, or $\text{H}_4\mathbf{1}^{6+} + \text{K}_7[\text{P}_2\text{W}_{17}\text{O}_{61}\text{Mn}(\text{H}_2\text{O})]$, or $\text{H}_4\mathbf{1}^{6+} + \text{K}_5\text{H}[\text{CoW}_{12}\text{O}_{40}]$ in HCl aq (pH 3.0). In the former two experiments, the total concentrations were set to be 3.0×10^{-6} M, the latter one was to be 2.8×10^{-6} M.

Determination of Association Constants of $\text{H}_2\mathbf{1}^{6+}$ with POMs.

A solution of $\text{H}_4\mathbf{1}^{6+}$ was titrated with those of POMs in HCl aq (pH 3.0) at room temperature. The absorbance changes at 485, 495, 505, 700, 710 and 720 nm were used for analysis of the association of $\text{H}_4\mathbf{1}^{6+}$ with $\text{K}_5\text{H}[\text{CoW}_{12}\text{O}_{40}]$, those at 485, 495, 505, 700, 710 and 720 nm for $\text{H}_4\mathbf{1}^{6+}$ with $\text{K}_6[\text{GeW}_{11}\text{O}_{39}\text{Mn}(\text{H}_2\text{O})]$, those at 475, 480, 485, 490, 495 and 500 nm for $\text{H}_4\mathbf{1}^{6+}$ with $\text{K}_7[\text{P}_2\text{W}_{17}\text{O}_{61}\text{Mn}(\text{H}_2\text{O})]$, those at 475, 485, 495, 700, 710 and 720 nm for $\text{H}_4\mathbf{1}^{6+}$ with $\text{K}_4[\text{PW}_{11}\text{O}_{39}\text{Mn}(\text{H}_2\text{O})]$, those at 475, 485, 495, 700, 710 and 720 nm for $\text{H}_4\mathbf{1}^{6+}$ with $\text{K}_5[\text{PW}_{11}\text{O}_{39}\text{Mn}(\text{H}_2\text{O})]$, those at 475, 480, 485, 490 and 495 nm for $\text{H}_4\mathbf{1}^{6+}$ with $\text{K}_6[\text{SiW}_{11}\text{O}_{39}\text{Mn}(\text{H}_2\text{O})]$ and those at 475, 480, 485, 490, 495 and 500 nm for $\text{H}_4\mathbf{1}^{6+}$ with $\text{K}_5[\text{SiW}_{11}\text{O}_{39}\text{Ru}(\text{H}_2\text{O})]$ (Ru-POM). The fittings of the plots were

performed using a nonlinear least-squares regression program¹² to obtain the association constants of H_4I^{6+} with the POMs.

Femtosecond Transient Absorption Measurements.

The source for the pump and probe pulses were derived from the fundamental output of Integra-C (780 nm, 2 mJ/pulse and fwhm = 130 fs) at a repetition rate of 1 kHz. A total of 75% of the fundamental output of the laser was introduced into TOPAS, which has optical frequency mixers resulting in tuneable range from 285 to 1660 nm, while the rest of the output was used for white-light generation. Prior to generating the probe continuum, a variable neutral density filter was inserted in the path to generate stable continuum, and then the laser pulse was fed to a delay line that provides an experimental time window of 3.2 ns with a maximum step resolution of 7 fs. In our experiments, a wavelength at 355 nm of TOPAS output, which is the fourth harmonic of signal or idler pulses, was chosen as the pump beam. As this TOPAS output consists of not only desirable wavelength but also unnecessary wavelengths, the latter was deviated using a wedge prism with wedge angle of 18°. The desirable beam was irradiated at the sample cell with a spot size of 1 mm diameter where it was merged with the white probe pulse in a close angle (< 10°). The probe beam after passing through the 2 mm sample cell was focused on a fibre optic cable that was connected to a CCD spectrograph for recording the time-resolved spectra (410 – 800 nm). Typically, 2500 excitation pulses were averaged for 5 s to obtain the transient spectrum at a set delay time. Kinetic traces at appropriate wavelengths were assembled from the time-resolved spectral data.

Nanosecond Transient Absorption Measurements.

Nanosecond time-resolved transient absorption measurements were performed using a laser system provided by UNISOKU Co., Ltd. The measurements were performed according to the following procedure: A deaerated solution was excited by a Panther optical parametric oscillator pumped by a Nd: YAG laser (Continuum, SLII-10, 4 – 6 ns fwhm) at $\lambda = 490$ and 500 nm. Photochemical reactions were monitored by continuous exposure to a xenon lamp (150 W) as a probe light and a photomultiplier tube (Hamamatsu 2949) as a detector.

Photocatalytic Reactions.

The photocatalytic oxidations of organic substrates were performed in a NMR tube containing an acidic D₂O solution (0.5 mL) of (H₄1)Cl₆ (5 μM), RuPOM (2 μM), Na₂S₂O₈ (2.2 mM) and a substrate (2.0 mM). The solution was irradiated with an ASAHI Spectra Co. Xe lamp MAX-300 (300 W), equipped with a band pass filter centred at 500 (ASAHI Spectra MX0500) or 710 nm (ASAHI Spectra MX0710). The tip of the light guide equipped on the light source were placed 2 cm away from the reaction vessel and the temperature around the vessel were monitored to keep the heat generated from the light source from heating the reaction vessel. The yield of the reaction products and the turnover numbers were determined by ¹H NMR spectroscopy.

The relative intensity of the irradiation light at 500 and 710 nm was estimated with a fluorescence method as describe below: at first, emission spectra of H₄1⁶⁺ upon irradiation of the light centred at 500 and 710 nm from the light source that was used for the photochemical oxidation (Fig. S19 in this ESI). The fluorescence intensity of H₄1⁶⁺ upon irradiating at 500 nm was 2.7 times larger than that at 710 nm, whereas the absorbance of H₄1⁶⁺ at 500 nm was 4.5 times larger than that at 710 nm. Therefore, the light intensity at 710 nm was 1.7 times larger than that at 500 nm.

Recyclability of the Photocatalyst.

A D₂O solution (1.0 mL, pD 3.0) containing H₄1⁶⁺ (5 μM), RuPOM (2 μM), Na₂S₂O₈ (2.2 mM), and MeBA (2.0 mM) was photoirradiated ($\lambda_{\text{centre}} = 500$ nm) at room temperature for 4 h. 4-Tolualdehyde as the oxidation product was quantified by ¹H NMR spectroscopy to be 0.28 μmol (14% yield against the substrate added and TON = 140). Then, further MeBA (2.1 mmol) and Na₂S₂O₈ (2.0 mmol) were added to the solution and photoirradiation ($\lambda_{\text{centre}} = 500$ nm) was conducted for 4 h, and increase of 4-tolualdehyde by 0.23 μmol (total TON for the two reactions: 252) was observed in the ¹H NMR spectrum of the solution. On the other hand, when the second run of the photocatalytic oxidation of MeBA was performed only with addition of MeBA but Na₂S₂O₈, only 0.01 μmol of 4-tolualdehyde was obtained, although the first run afforded 0.27 μmol of 4-tolualdehyde. Therefore, addition of Na₂S₂O₈ is indispensable on and after the second run of the photocatalytic reaction.

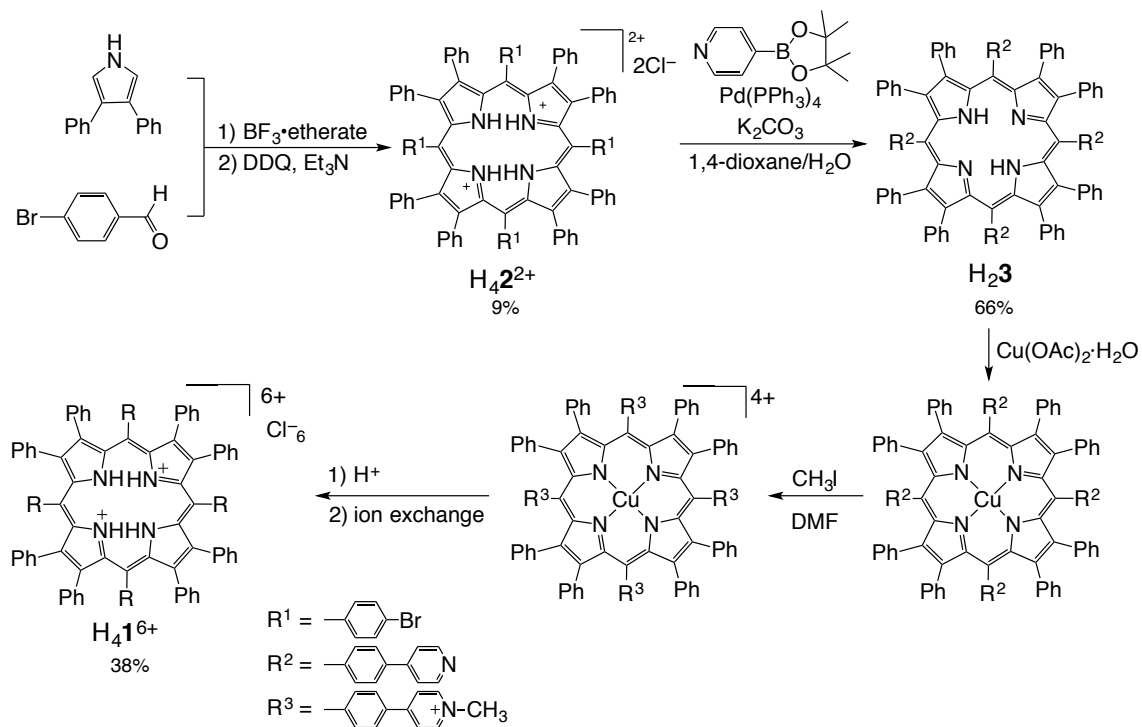
Determination of the Quantum Yield for the Photocatalytic Oxidation of MeBA Catalysed by $(\text{H}_4\mathbf{1}^{6+})_2\text{-RuPOM}$.

The measurement to determine the quantum yields (Φ) was performed in a quartz cuvette (path length: 1 cm) containing an acidic D_2O solution (3 mL) of $\text{H}_4\mathbf{1}^{6+}$ (5 μM), RuPOM (2 μM), $\text{S}_2\text{O}_8^{2-}$ (2.2 mM) and 4-methylbenzyl alcohol (MeBA, 2.0 mM). The solution was irradiated with an ASAHI Spectra Co. Xe lamp MAX-300, equipped with a band pass filter centred at 500 nm. The incident light intensity was determined using a $\text{K}_3\text{Fe}(\text{C}_2\text{O}_4)_3$ actinometer to be 3.62×10^{-9} einstein s^{-1} . The quantity of the reaction product (4-methyl-benzaldehyde) was determined by ^1H NMR spectroscopy to be 0.144 μmol after 1 h photoirradiation. Φ was defined as [product / mol]/[absorbed photon / einstein] (the internal quantum yield) and the absorbance at 500 nm for the sample solution was 0.431.

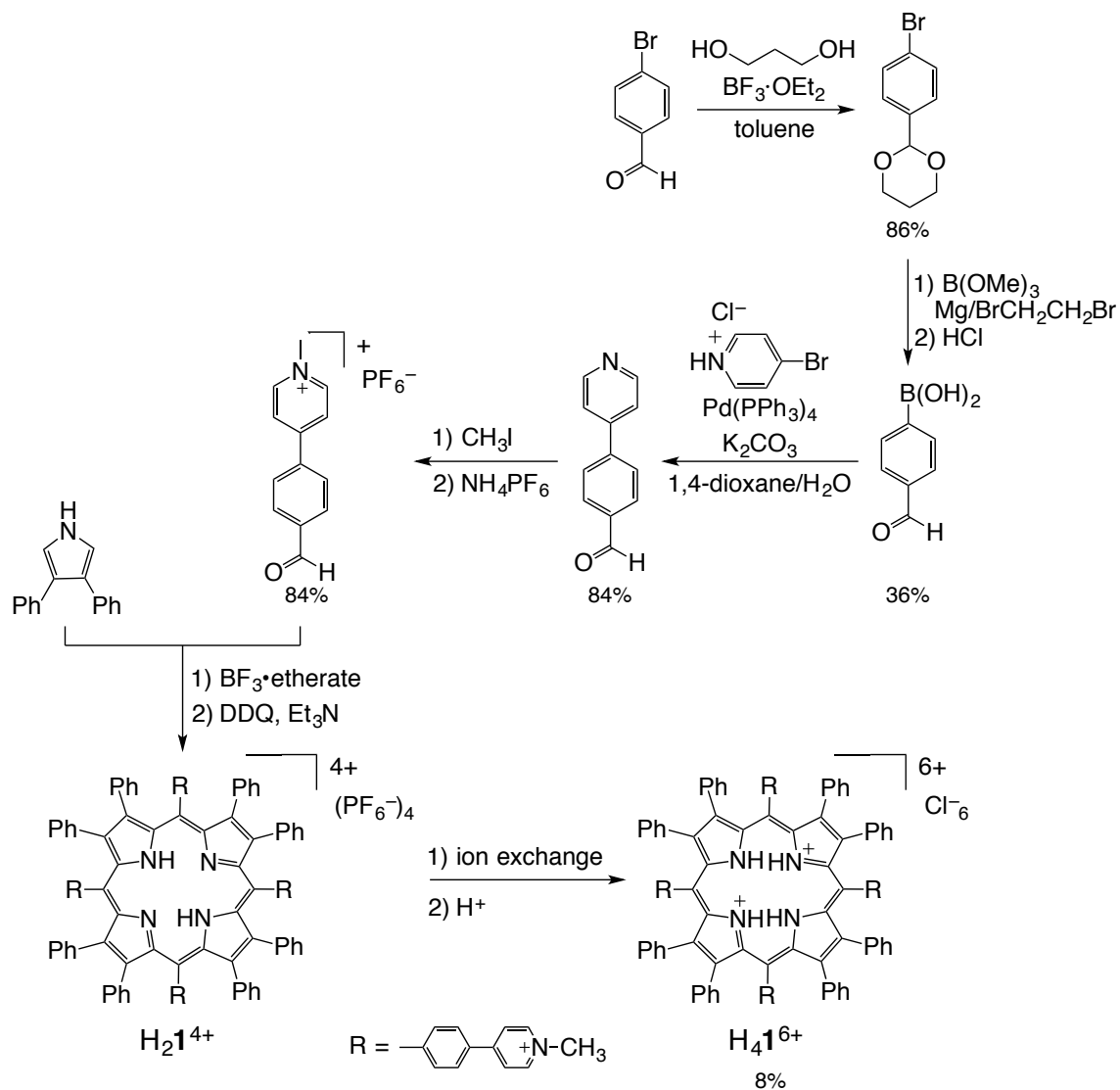
Reference and Notes

- S1 E. N. Glass, J. Fielden, A. L. Kaledin, D. G. Musaev, T. Q. Lian and C. L. Hill, *Chem.–Eur. J.*, 2014, **20**, 4297.
- S2 C. Tourné, G. Tourné, S. A. Malik and T. J. R. Weakley, *J. Inorg. Nucl. Chem.*, 1970, **32**, 3875.
- S3 D. K. Lyon, W. K. Muller, T. Novet, P. J. Domaille, E. Evitt, D. C. Johnson and R. G. Finke, *J. Am. Chem. Soc.*, 1991, **113**, 7209.
- S4 M. Sadakane, D. Tsukuma, M. H. Dickman, B. Bassil, U. Kortz, M. Higashijima and W. Ueda, *Dalton Trans.*, 2006, 4271.
- S5 P. Gu, Y. Su, X. Wu, J. Sun, W. Liu, P. Xue and R. Li, *Org. Lett.* **2012**, *14*, 2246.
- S6 F. Chen, T. Shen, Y. Cui and N. Jiao, *Org. Lett.*, 2012, **14**, 4926.
- S7 K. Perie, J.-M. Barbe, P. Cocolios and R. Guillard, *Bull. Soc. Chim. Fr.* **1996**, *133*, 697.
- S8 D. Wu, T. Shao, J. Men, X. Chen and G. Gao, *Dalton Trans.*, 2014, **43**, 1753.
- S9 D. Trawny, L. Vandromme, J. P. Rabe and H. U. Reissig, *Eur. J. Org. Chem.*, 2014, 4985.
- S10 G. M. Sheldrick, SIR97 and SHELX97, Programs for Crystal Structure Refinement, University of Göttingen, Göttingen (Germany), 1997.
- S11 P. V. C. Sluis and A. L. Spek, *Acta. Crystallogr.*, 1990, **A46**, 194.
- S12 K. Hirose, *Incl. Phenom. Macrocycl. Chem.*, 2001, **39**, 193.

Scheme S1 Synthetic route 1 for $[H_41^{6+}]Cl_6$.



Scheme S2 Synthetic route 2 for $[H_4\mathbf{1}^{6+}]Cl_6$.



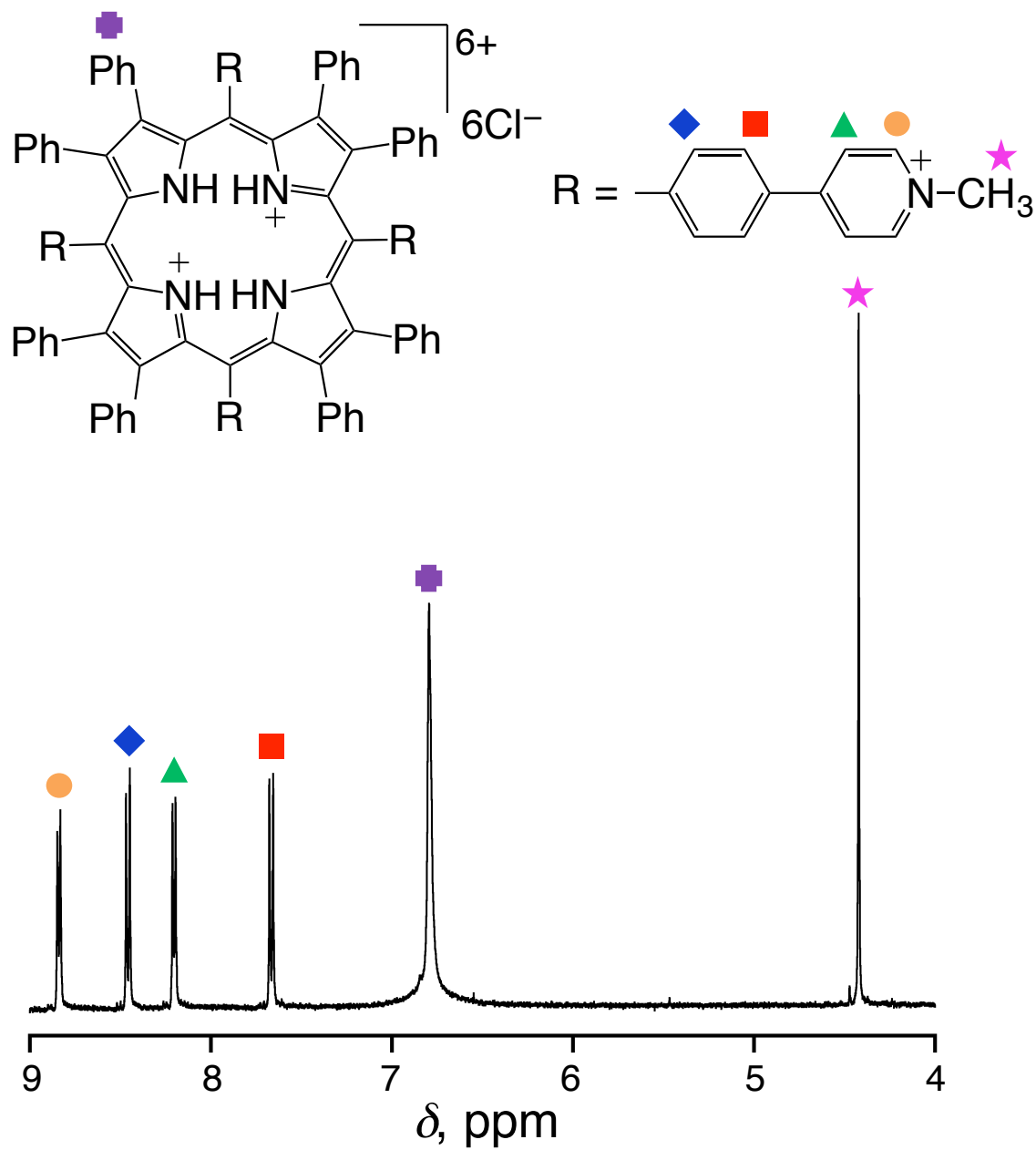


Fig. S1 ^1H NMR spectrum of $\text{H}_4\text{1}^{6+}$ in CD_3CN .

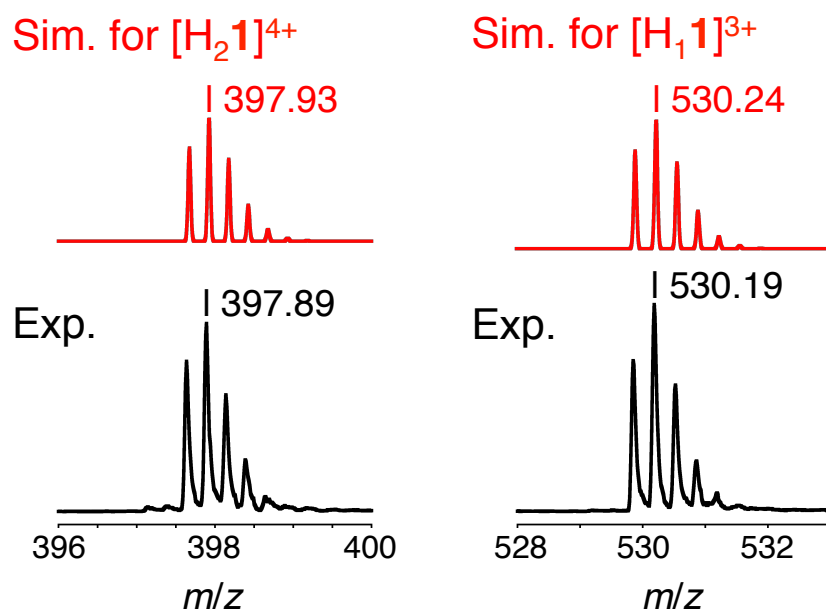


Fig. S2 An ESI-TOF-MS spectrum of H_21^{4+} in MeOH (black) and its simulation (red).

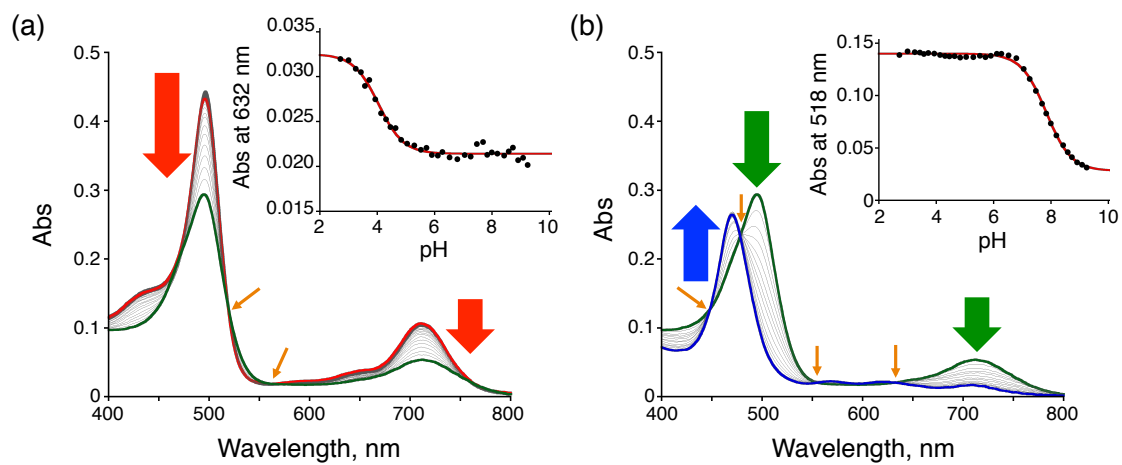


Fig. S3 UV-Vis spectral changes of H_4I^{6+} (3.3 μM) in the course of pH titration in hexamine buffer: pH 2.71 – 6.52 (a) and pH 6.52 – 9.24 (b). Insets: analysis of the absorbance changes at 632 nm (c) and 518 nm (d) with pH titration. The orange arrows in (a) and (b) indicate the isosbestic points: 518 and 561 nm for (a) and 446, 479, 559 and 632 nm for (b).

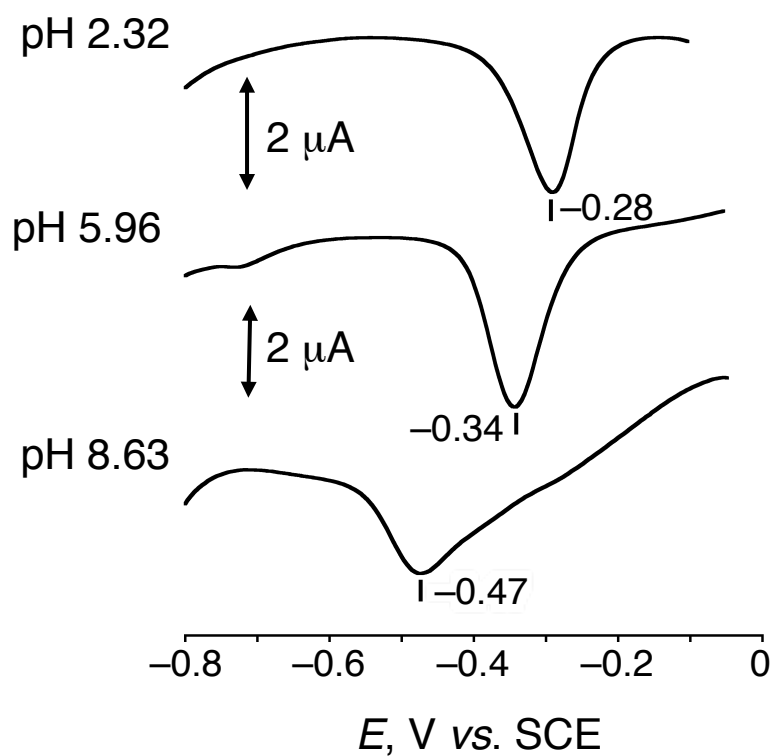


Fig. S4 DPV traces of H_4I^{6+} (0.1 mM) in hexamine buffer, containing 0.1 M NaCl as an electrolyte, under Ar at 298 K. The solution pH was controlled by addition of NaOH aq (15 M).

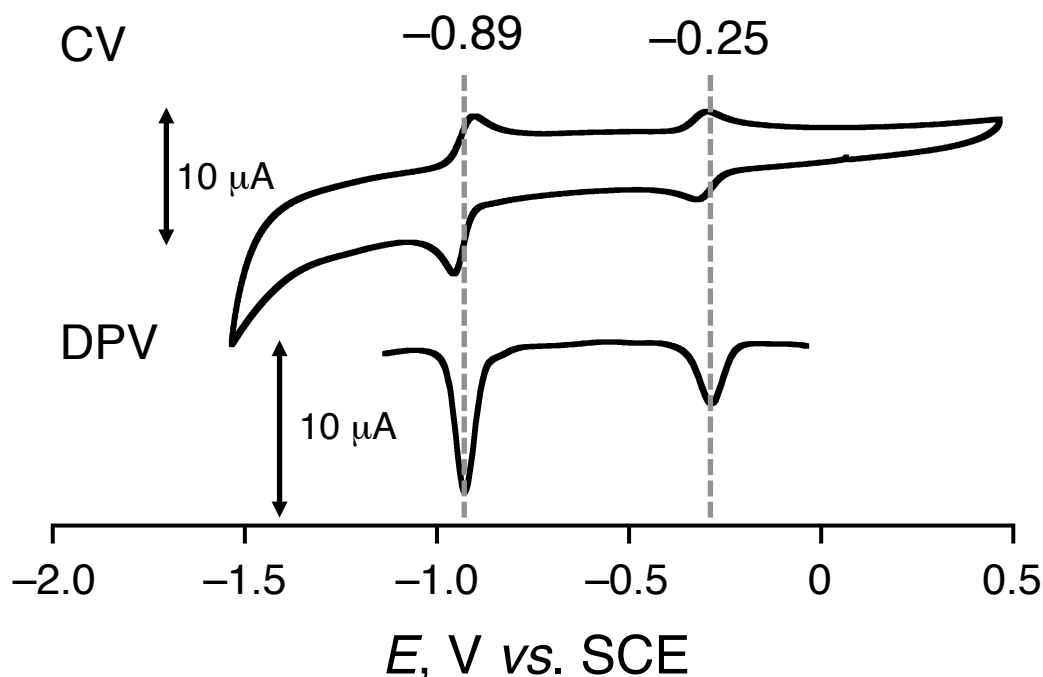


Fig. S5 CV and DPV of $\text{H}_4\mathbf{1}^{6+}$ (0.7 mM) in MeCN containing 0.1 M $(n\text{-Bu})_4\text{N}^+\text{PF}_6^-$ as an electrolyte under Ar at 298 K.

Two reversible waves were observed at -0.25 and -0.89 V vs. SCE, which were assigned to the reduction processes of the porphyrin core and the *N*-methyl-pyridiniumyl groups (B. M. L. Chen and A. Tulinsky, *J. Am. Chem. Soc.*, 1972, **94**, 4144). The current ratio between the waves at -0.25 and -0.89 V was estimated to be 1:2, and the latter should be $4e^-$ -process, since there are four *N*-methyl-pyridiniumyl groups. Therefore, the former redox process can be assigned to $2e^-$ -reduction process of the porphyrin core of $\text{H}_4\mathbf{1}^{6+}$ through disproportionation of $2\text{H}_4\mathbf{1}^{5+} \rightarrow \text{H}_4\mathbf{1}^{4+} + \text{H}_4\mathbf{1}^{6+}$. See: T. Nakanishi, K. Ohkubo, T. Kojima and S. Fukuzumi, *J. Am. Chem. Soc.*, 2009, **131**, 577.

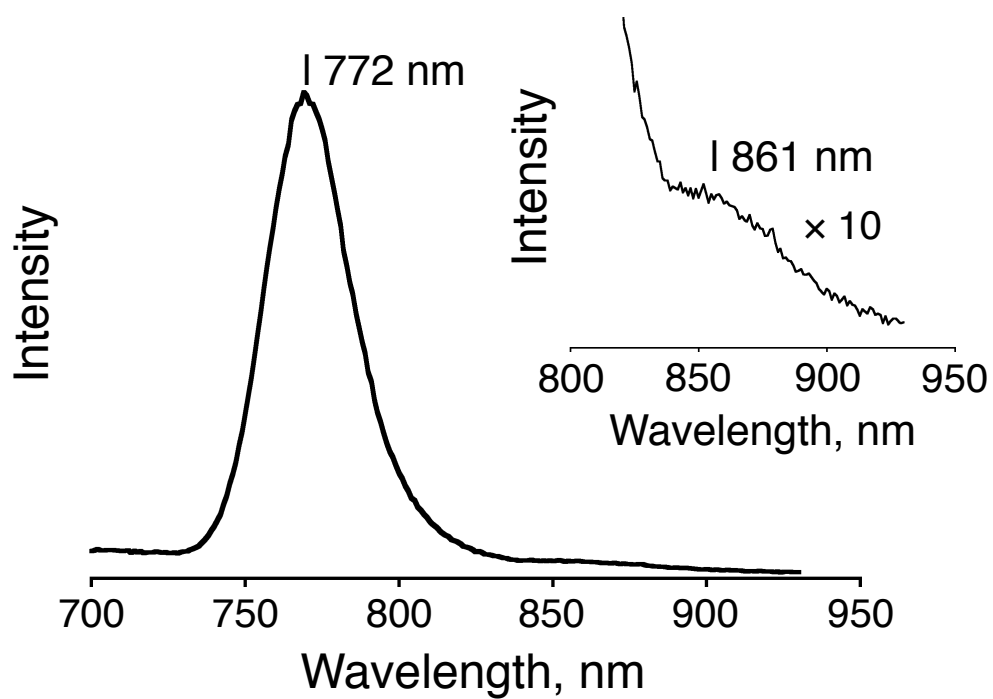


Fig. S6 Emission spectrum of H_4I^{6+} (10 μM) in EtOH containing an aliquot of *conc.* HCl at 77 K under Ar ($\lambda_{\text{ex}} = 500$ nm).

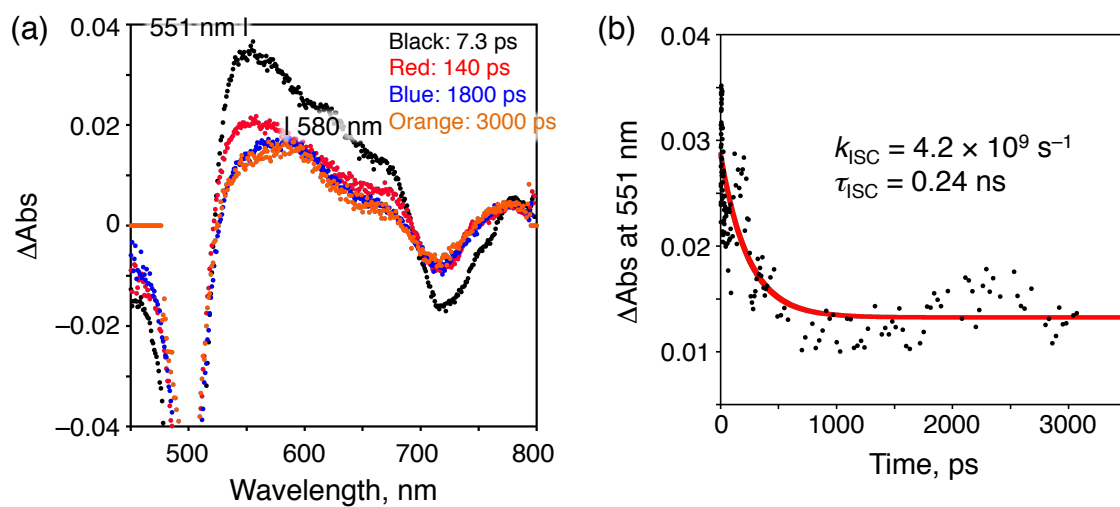


Fig. S7 (a) Time-resolved femtosecond transient absorption spectra ($\lambda_{\text{ex}} = 500$ nm) of H41^{6+} (21 μM) in HCl aq (pH 1.6) under Ar. (b) Decay of the absorbance at 551 nm and the single-exponential analysis (red solid line).

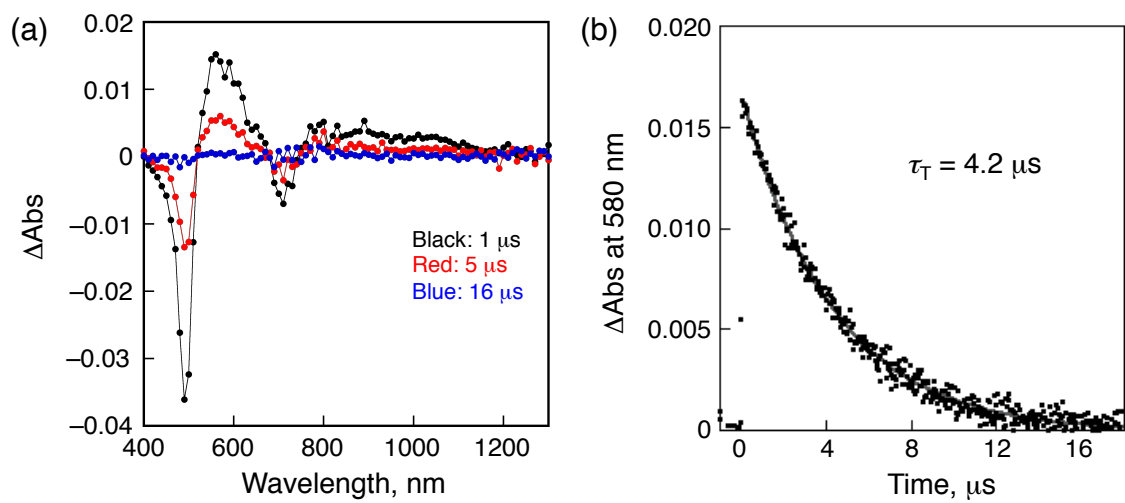


Fig. S8 (a) Time-resolved nanosecond transient absorption spectra ($\lambda_{ex} = 430$ nm) of H_41^{6+} (0.50 mM) in HCl aq (pH 3) under Ar. (b) Decay of the absorbance at 580 nm and single-exponential curve fitting (grey solid line).

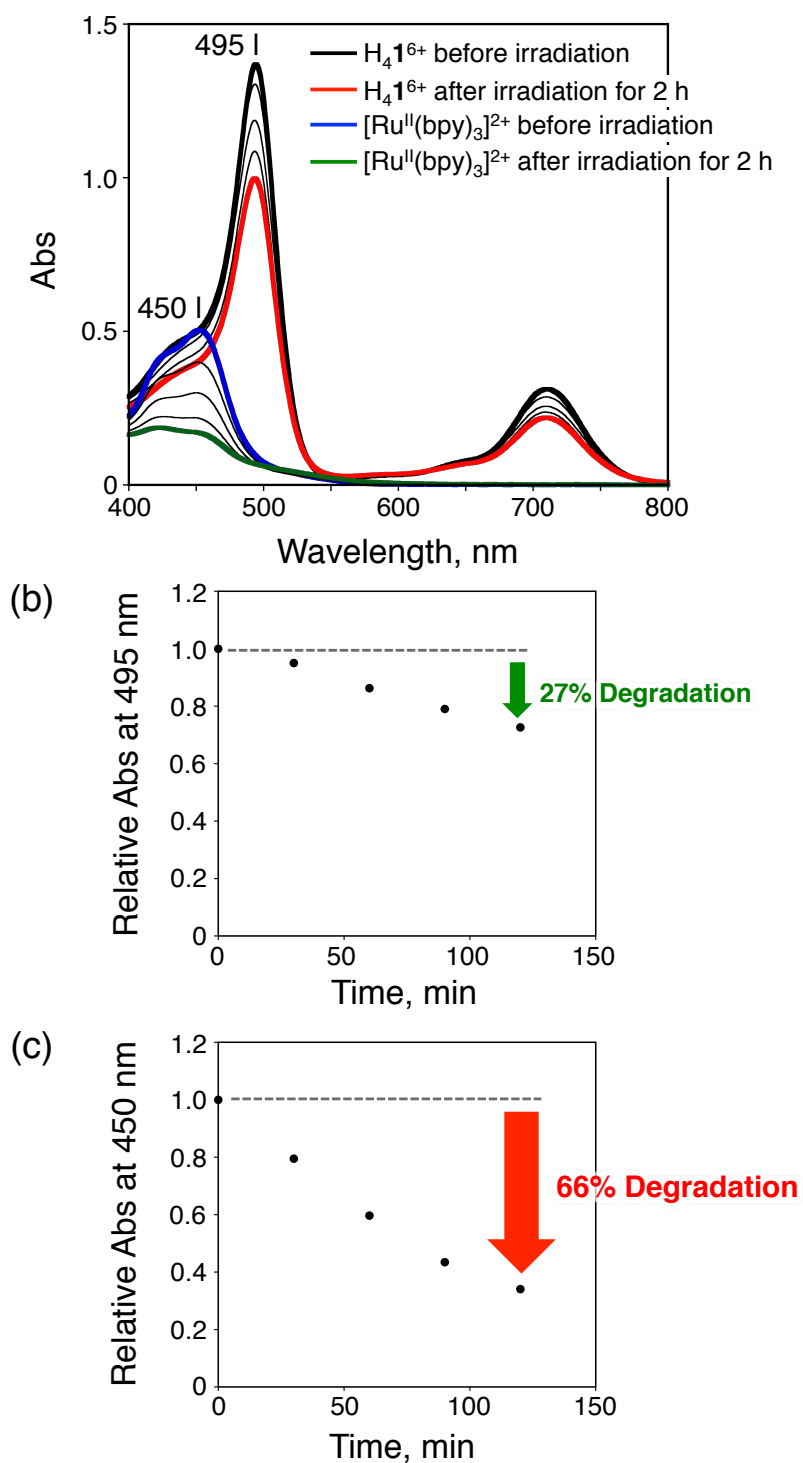


Fig. S9 (a) UV-Vis spectral changes of H_41^{6+} and $[Ru(bpy)_3]^{2+}$ upon photoirradiation ($\lambda_{irr} = 450$ nm) in acidic water (pH 3.0) at room temperature under Ar. The absorbance decreases due to the photodegradation of H_41^{6+} at 495 nm (b) and of $[Ru(bpy)_3]^{2+}$ at 450 nm (c).

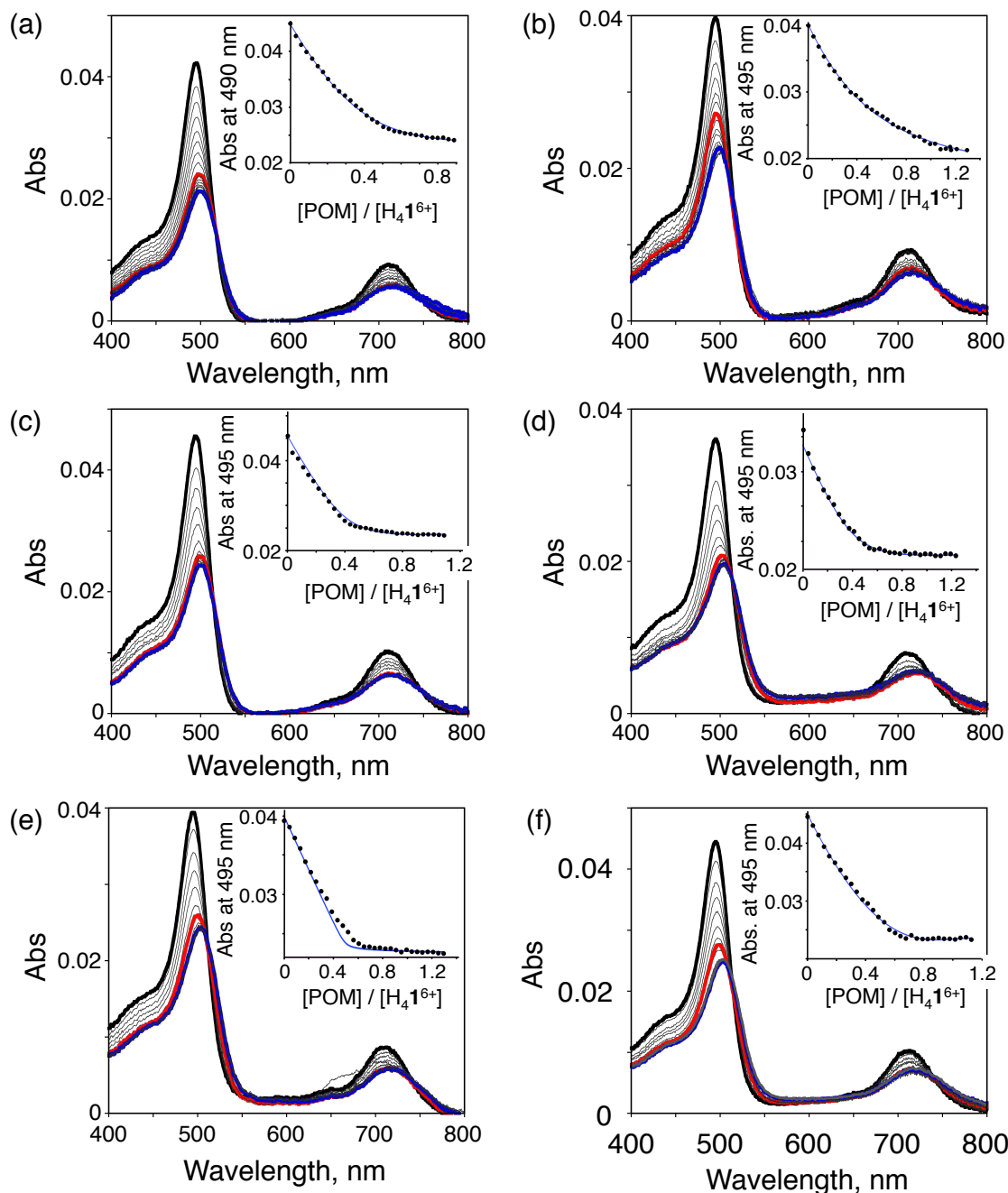


Fig. S10 UV-Vis titration of $[\text{H}_4\text{I}^{6+}]\text{Cl}_6$ with $\text{K}_5\text{H}[\text{CoW}_{12}\text{O}_{40}]$ (a), $\text{K}_6[\text{GeW}_{11}\text{O}_{39}\text{Mn}(\text{H}_2\text{O})]$ (b), $\text{K}_7[\text{P}_2\text{W}_{17}\text{O}_{61}\text{Mn}(\text{H}_2\text{O})]$ (c), $\text{K}_4[\text{PW}_{11}\text{O}_{39}\text{Mn}(\text{H}_2\text{O})]$ (d), $\text{K}_5[\text{PW}_{11}\text{O}_{39}\text{Mn}(\text{H}_2\text{O})]$ (e), and $\text{K}_6[\text{SiW}_{11}\text{O}_{39}\text{Mn}(\text{H}_2\text{O})]$ (f) in HCl aq (pH 3.0) at 298 K. $[\text{H}_4\text{I}^{6+}] = 3.4 \times 10^{-7}$ M for (a), 3.1×10^{-7} M for (b), 3.6×10^{-7} M for (c), 2.8×10^{-7} M for (d), 3.1×10^{-7} M for (e), and 3.5×10^{-7} M for (f). Inset: Absorbance changes of H_4I^{6+} at 490 nm for (a) and 495 nm for (b – f) upon the titrations.

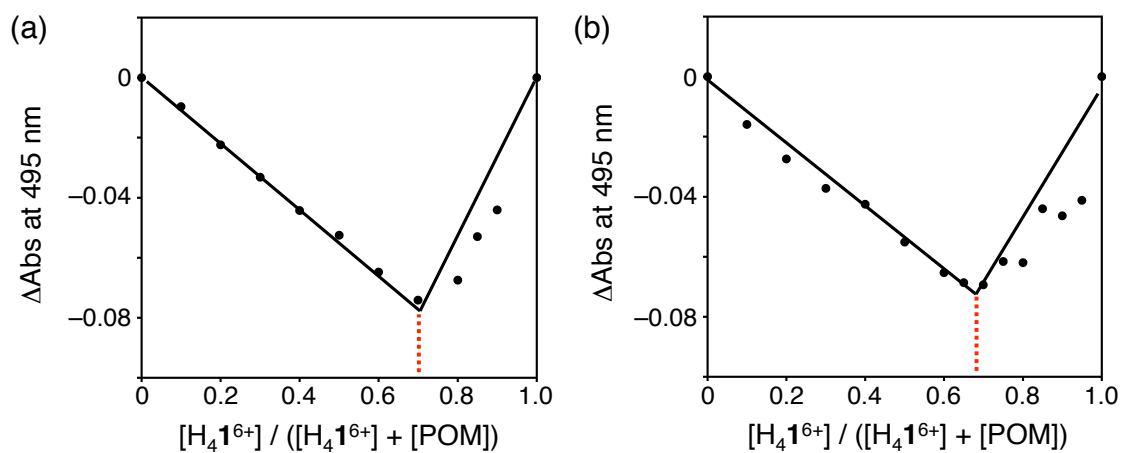


Fig. S11 Job's plots for the association equilibrium of (a) $\text{H}_4\mathbf{1}^{6+}$ and $\text{K}_5\text{H}[\text{CoW}_{12}\text{O}_{40}]$ and (b) $\text{H}_4\mathbf{1}^{6+}$ and $\text{K}_7[\text{P}_2\text{W}_{17}\text{O}_{61}\text{Mn}(\text{H}_2\text{O})]$. The absorbance changes at 495 nm were used for the plots. The total concentrations of $\text{H}_4\mathbf{1}^{6+}$ and POMs were set to be 2.8×10^{-6} M for (a) and 3.0×10^{-6} M for (b).

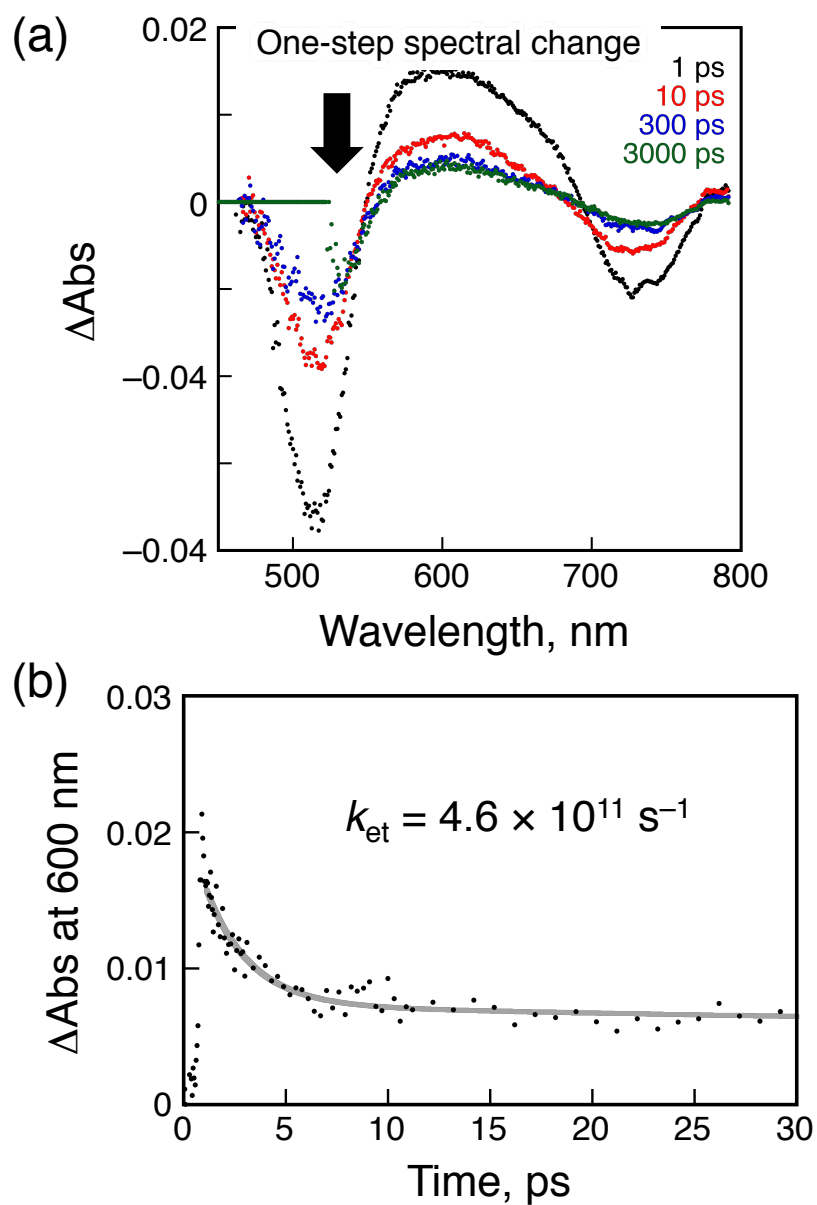


Fig. S12 (a) Time-resolved fs-transient absorption spectra ($\lambda_{\text{ex}} = 393 \text{ nm}$) of the supramolecular complex, $(\text{H}_4\mathbf{1}^{6+})_2\text{-RuPOM}$, in deaerated HCl aq (pH 3) at 298 K. $[\text{H}_4\mathbf{1}^{6+}] = 0.50 \text{ mM}$, $[\text{RuPOM}] = 0.30 \text{ mM}$. (b) Decay of the absorbance at 600 nm and the single-exponential curve fitting (grey solid line).

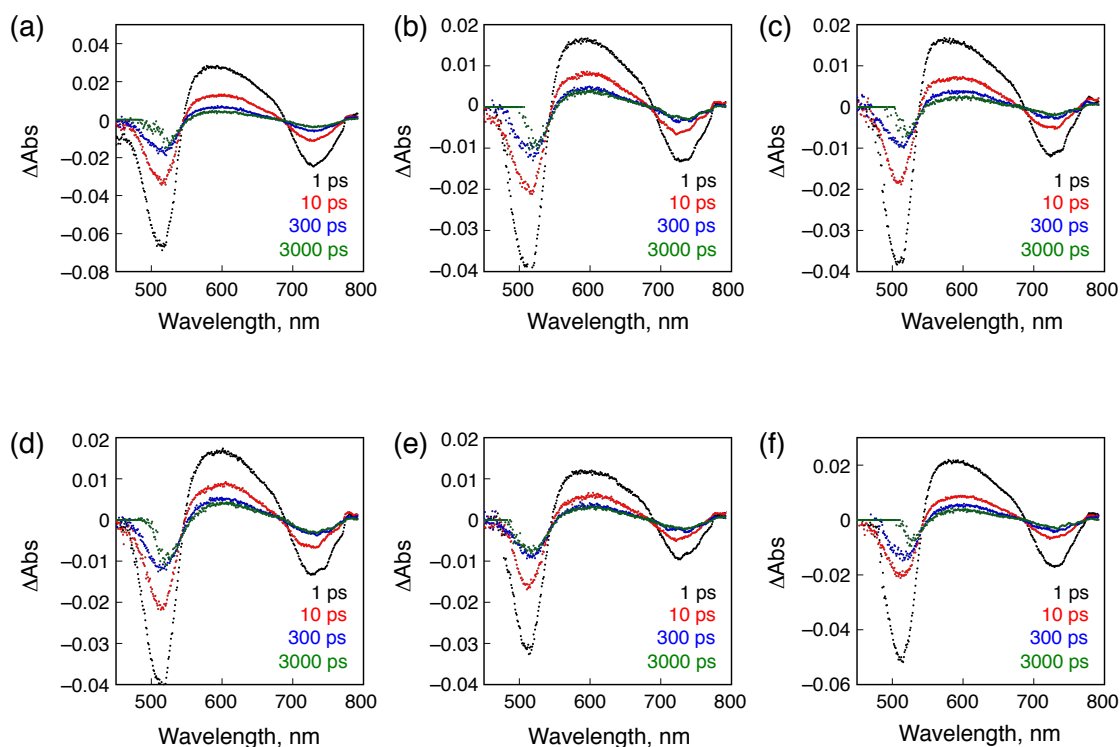


Fig. S13 Time-resolved fs-transient absorption spectra of the supramolecular complexes, $(\text{H}_4\mathbf{1}^{6+})_2\text{-POM}$, ($\lambda_{\text{ex}} = 393 \text{ nm}$) at 298 K; (a) $[\text{H}_4\mathbf{1}^{6+}] = 0.25 \text{ mM}$ and $[\text{K}_5\text{H}[\text{CoW}_{12}\text{O}_{40}]] = 80 \text{ }\mu\text{M}$, (b) $[\text{H}_4\mathbf{1}^{6+}] = 0.30 \text{ mM}$ and $[\text{K}_6[\text{GeW}_{11}\text{O}_{39}\text{Mn}(\text{H}_2\text{O})]] = 0.10 \text{ mM}$, (c) $[\text{H}_4\mathbf{1}^{6+}] = 0.30 \text{ mM}$ and $[\text{K}_7[\text{P}_2\text{W}_{17}\text{O}_{61}\text{Mn}(\text{H}_2\text{O})]] = 0.10 \text{ mM}$, (d) $[\text{H}_4\mathbf{1}^{6+}] = 0.50 \text{ mM}$ and $[\text{K}_4[\text{PW}_{11}\text{O}_{39}\text{Mn}(\text{H}_2\text{O})]] = 0.25 \text{ mM}$, (e) $[\text{H}_4\mathbf{1}^{6+}] = 0.50 \text{ mM}$ and $[\text{K}_5[\text{PW}_{11}\text{O}_{39}\text{Mn}(\text{H}_2\text{O})]] = 0.30 \text{ mM}$ and (f) $[\text{H}_4\mathbf{1}^{6+}] = 0.50 \text{ mM}$ and $[\text{K}_6[\text{SiW}_{11}\text{O}_{39}\text{Mn}(\text{H}_2\text{O})]] = 0.25 \text{ mM}$.

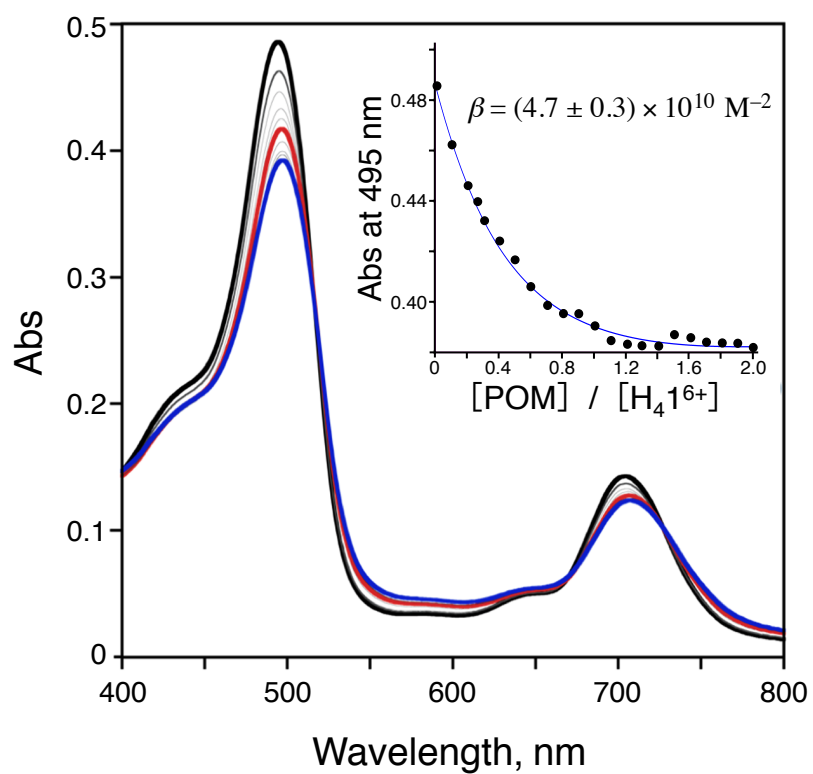


Fig. S14 UV-Vis titration of $[H_4I^{6+}]Cl_6$ with RuPOM in HCl aq (pH 3.0) containing $Na_2S_2O_8$ (2.2 mM) at 298 K. $[H_4I^{6+}] = 5.0 \mu M$. Inset: Absorbance changes of H_4I^{6+} at 495 nm upon the titration.

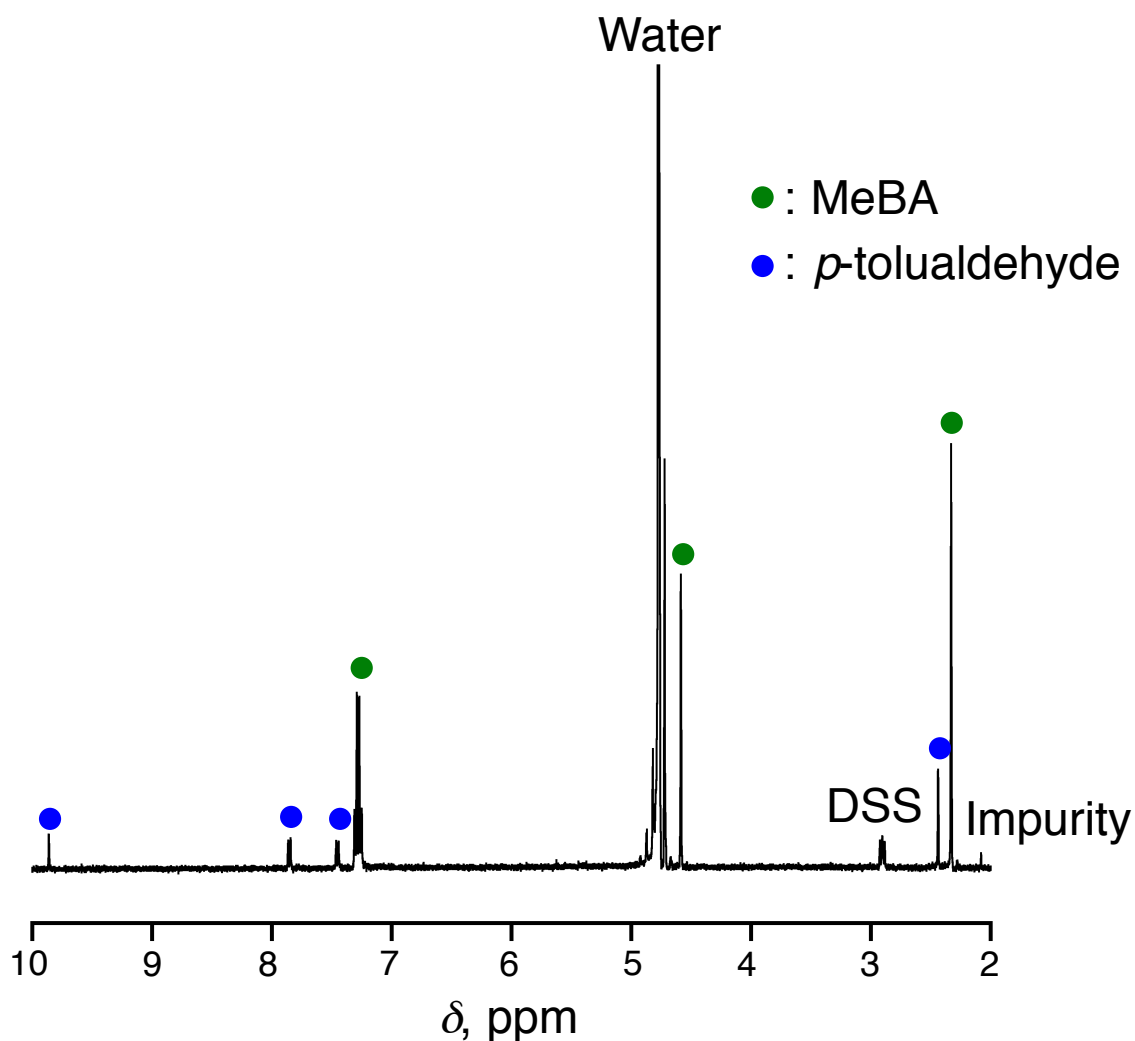


Fig. S15 ^1H NMR spectrum of a reaction mixture of the photocatalytic oxidation of MeBA using $\text{H}_4\mathbf{1}^{6+}$ as a photosensitizer, RuPOM as a catalyst, and $\text{Na}_2\text{S}_2\text{O}_8$ as a sacrificial oxidant. The reaction was performed under photoirradiation with a Xe lamp (300 W) equipped with a band-pass filter ($\lambda_{\text{center}} = 500 \text{ nm}$) for 4 h. Green filled circles: MeBA. Blue filled circles: *p*-tolualdehyde. Reaction conditions: $[\text{RuPOM}] = 2 \mu\text{M}$, $[\text{H}_4\mathbf{1}^{6+}] = 5 \mu\text{M}$, $[\text{Na}_2\text{S}_2\text{O}_8] = 2.2 \text{ mM}$, $[\text{MeBA}] = 12.0 \text{ mM}$. Solvent: D_2O acidified with HCl (pD 3.0). Temperature: 298 K.

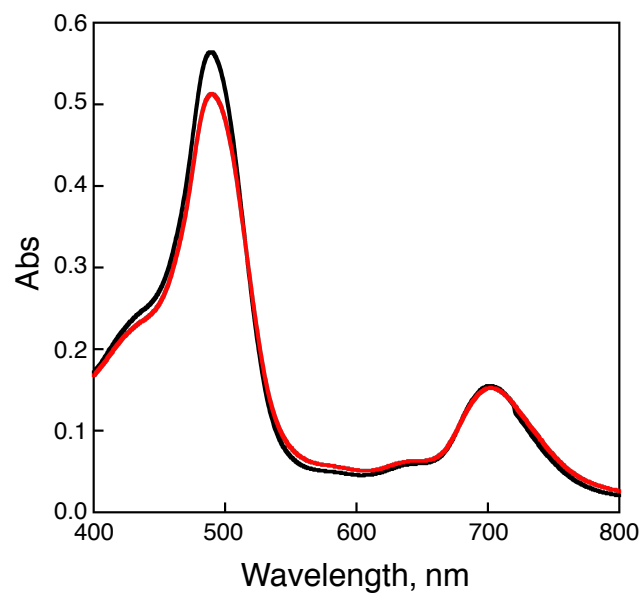


Fig. S16 UV-Vis spectra of the reaction solution containing $\text{H}_4\mathbf{1}^{6+}$ ($5\ \mu\text{M}$), RuPOM ($2\ \mu\text{M}$), $\text{Na}_2\text{S}_2\text{O}_8$ ($2.2\ \text{mM}$) and MeBA ($2.0\ \text{mM}$) before (black) and after photoirradiation for 4 h centred at 500 nm (red).

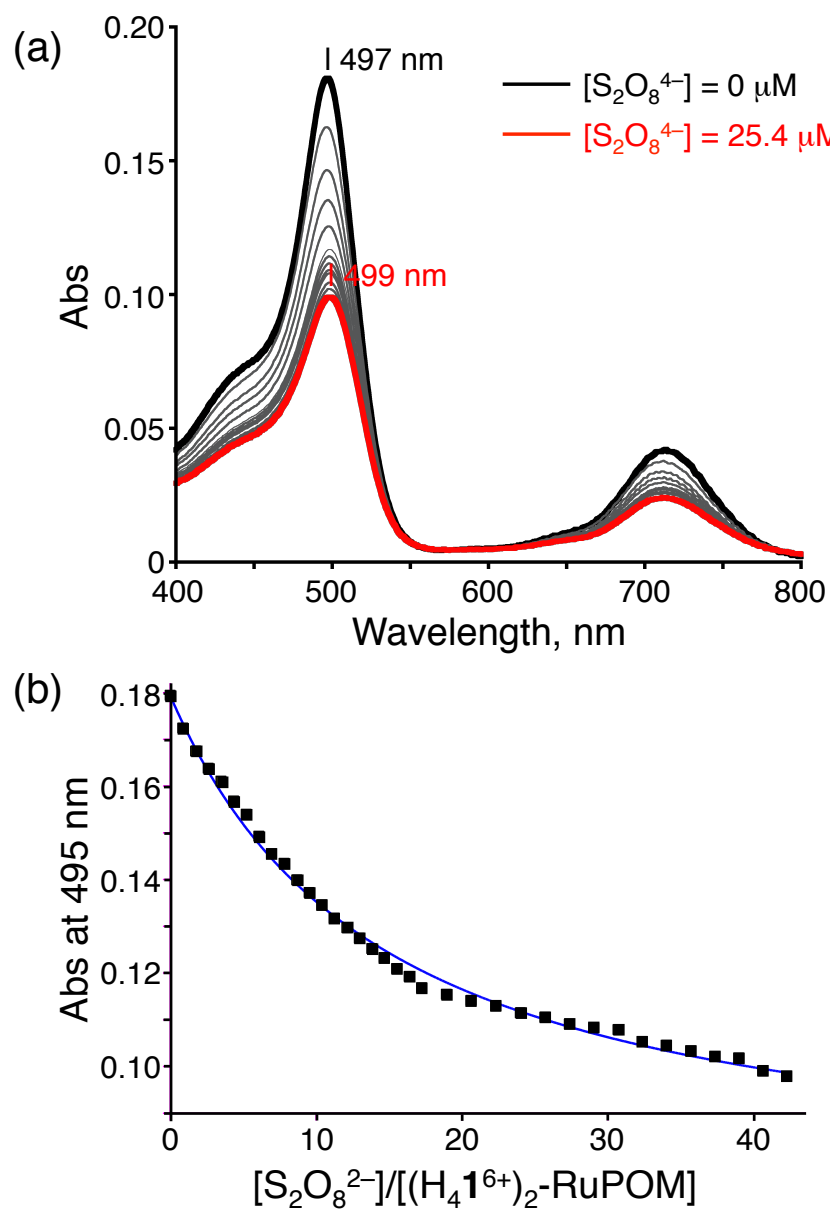


Fig. S17 (a) UV-Vis titration of $(\text{H}_4\text{I}^{6+})_2\text{-RuPOM}$ with $\text{S}_2\text{O}_8^{2-}$ in HCl aq (pH 3.0) at 298 K: $[\text{H}_4\text{I}^{6+}]_0 = 1.25 \mu\text{M}$, $[\text{RuPOM}]_0 = 0.625 \mu\text{M}$. (b) Absorbance change at 495 nm upon titration with $\text{S}_2\text{O}_8^{2-}$ and the fitting curve based on 1:1 association equilibrium.

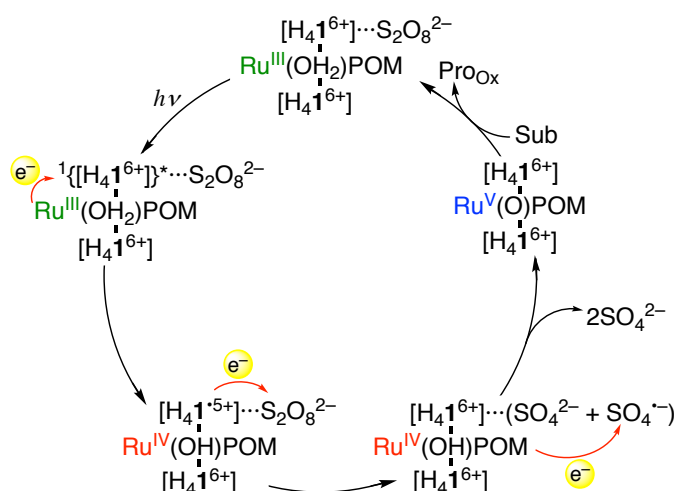


Fig. S18 A proposed reaction mechanism for the photocatalytic substrate oxidation using $(\text{H}_4\mathbf{1}^{6+})_2\text{-RuPOM}$ as a photocatalyst.

For the first step, one of the $\text{H}_4\mathbf{1}^{6+}$ components is photoexcited to form ${}^1(\text{H}_4\mathbf{1}^{6+})^*$ and ISET occurs from RuPOM to ${}^1(\text{H}_4\mathbf{1}^{6+})^*$ to give $\text{S}_2\text{O}_8^{2-}\cdots(\text{H}_4\mathbf{1}^{6+})(\text{H}_4\mathbf{1}^{5+})\text{-RuPOM}_{\text{ox}}$, which probably includes a Ru^{IV} centre. $\text{H}_4\mathbf{1}^{5+}$ obtained undergoes ISET to $\text{S}_2\text{O}_8^{2-}$ to afford $(\text{H}_4\mathbf{1}^{6+})_2\text{-RuPOM}_{\text{ox}}$. The $1e^-$ -reduced $\text{S}_2\text{O}_8^{2-}$ immediately decomposes into SO_4^{2-} and highly reactive $\text{SO}_4^{\bullet-}$ (C. Dai, F. Meschini, J. M. R. Narayanam and C. R. J. Stephenson, *J. Org. Chem.*, 2012, **77**, 4425). $\text{SO}_4^{\bullet-}$ formed further oxidizes RuPOM_{ox} to afford a putative active species, $\text{O}=\text{Ru}^{\text{V}}(\text{POM})$ (R. Neumann and C. Abu.-Gnim, *J. Am. Chem. Soc.*, 1990, **112**, 6025; M. Murakami, D. Hong, T. Suenobu, S. Yamaguchi, T. Ogura and S. Fukuzumi, *J. Am. Chem. Soc.*, 2011, **133**, 11605).^{14,15} Therefore, in this catalytic cycle, a one-photon/ $2e^-$ process should proceed due to the formation of a multicomponent supramolecular assembly including $\text{S}_2\text{O}_8^{2-}$ as a potential $2e^-$ oxidant.

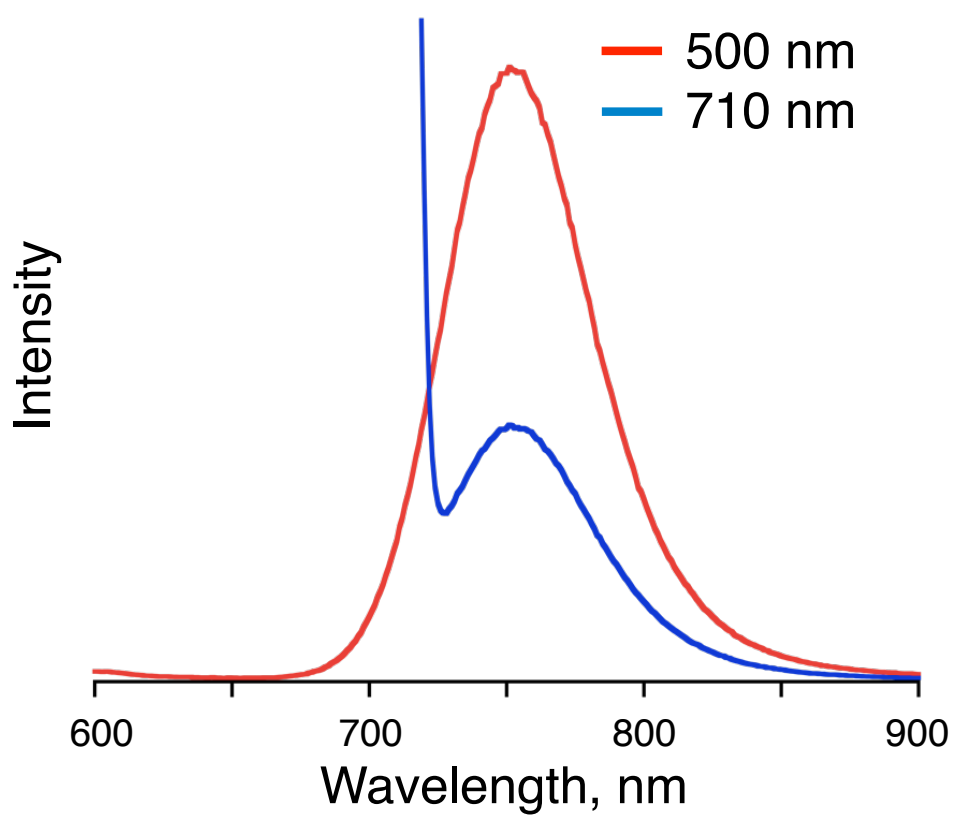


Fig. S19 Emission spectra of H_4I^{6+} ($2 \mu\text{M}$) in HCl aq (pH 3.0) at 298 K upon irradiation with a Xe lamp (ASAHI Spectra MAX-300) equipped with a band path filter centred at 500 nm (blue) and 710 nm (red).

Table S1 Summary of global association constants, β , for the association of $[\text{H}_4\mathbf{1}^{6+}]\text{Cl}_6$ with POM, $1e^-$ -oxidation potential (E_{ox}) of POM, driving force of electron transfer ($-\Delta G_{\text{et}}$ and $-\Delta G_{\text{bet}}$) and rate constants (k_{et}) of intrasupramolecular photoinduced electron transfer from POM to $[\text{H}_4\mathbf{1}^{6+}]\text{Cl}_6$ in HCl aq (pH 3) at 298 K

POM	$\beta,^a \text{M}^{-2}$	E_{ox}^b	$-\Delta G_{\text{et}}^c$	$-\Delta G_{\text{bet}}^d$	k_{et}^e
$\text{K}_3\text{H}[\text{CoW}_{12}\text{O}_{40}]$	$(9.7 \pm 2.9) \times 10^{13}$	+0.81	0.58	1.09	4.2
$\text{K}_6[\text{GeW}_{11}\text{O}_{39}\text{Mn}(\text{H}_2\text{O})]$	$(2.0 \pm 0.8) \times 10^{13}$	+0.57	0.82	0.85	3.1
$\text{K}_7[\text{P}_2\text{W}_{17}\text{O}_{61}\text{Mn}(\text{H}_2\text{O})]$	$(4.0 \pm 1.1) \times 10^{14}$	+0.45	0.94	0.73	3.1
$\text{K}_4[\text{PW}_{11}\text{O}_{39}\text{Mn}(\text{H}_2\text{O})]$	$(4.7 \pm 1.2) \times 10^{14}$	+0.61	0.78	0.89	5.8
$\text{K}_5[\text{PW}_{11}\text{O}_{39}\text{Mn}(\text{H}_2\text{O})]$	$(3.7 \pm 1.4) \times 10^{16}$	+0.62	0.77	0.90	4.0
$\text{K}_6[\text{SiW}_{11}\text{O}_{39}\text{Mn}(\text{H}_2\text{O})]$	$(1.8 \pm 0.6) \times 10^{15}$	+0.45	0.94	0.73	3.8
$\text{K}_5[\text{SiW}_{11}\text{O}_{39}\text{Ru}(\text{H}_2\text{O})]$ (Ru-POM)	$(3.8 \pm 1.7) \times 10^{14}$	+0.59	0.80	0.87	4.6

^a Overall association constant (M^{-2}) with $\text{H}_4\mathbf{1}^{6+}$ by the 1:2 molecular ratio. ^b in V vs. SCE.

^c $e[E_{\text{red}}(\text{H}_4\mathbf{1}^{6+}) - E_{\text{ox}}(\text{POM})]$, eV. ^d $e[E_{\text{ox}}(\text{POM}) - E_{\text{red}}(\text{H}_4\mathbf{1}^{6+})]$, eV. ^e in 10^{11}s^{-1}

Table S2 Summary of IR vibration bands of supramolecular assemblies

	ν, cm^{-1}					
$\{(\text{H}_4\mathbf{1})_2[\text{CoW}_{12}\text{O}_{40}]\}^{6+}$	3051	1635	—	932	869	759
$\text{K}_5\text{H}[\text{CoW}_{12}\text{O}_{40}]^a$	—	—	—	943	877	761
$\{(\text{H}_4\mathbf{1})_2[\text{GeW}_{11}\text{O}_{39}\text{Mn}(\text{H}_2\text{O})]\}^{6+}$	3047	1636	1473	945	879	810
$\text{K}_6[\text{GeW}_{11}\text{O}_{39}\text{Mn}(\text{H}_2\text{O})]$	—	—	—	954	875	813
$\{(\text{H}_4\mathbf{1})_2[\text{P}_2\text{W}_{17}\text{O}_{61}\text{Mn}(\text{H}_2\text{O})]\}^{5+}$	3047	1634	1083	1012	946	912
$\text{K}_7[\text{P}_2\text{W}_{17}\text{O}_{61}\text{Mn}(\text{H}_2\text{O})]^b$	—	—	1086	1015	951	915
$\{(\text{H}_4\mathbf{1})_2[\text{PW}_{11}\text{O}_{39}\text{Mn}(\text{H}_2\text{O})]\}^{8+}$	3047	1636	1295	1075	961	881
$\text{K}_4[\text{PW}_{11}\text{O}_{39}\text{Mn}(\text{H}_2\text{O})]$	—	—	1384	1081	973	882
$\{(\text{H}_4\mathbf{1})_2[\text{PW}_{11}\text{O}_{39}\text{Mn}(\text{H}_2\text{O})]\}^{7+}$	3041	1636	1075	1048	949	883
$\text{K}_5[\text{PW}_{11}\text{O}_{39}\text{Mn}(\text{H}_2\text{O})]$	—	—	1078	1052	958	889
$\{(\text{H}_4\mathbf{1})_2[\text{SiW}_{11}\text{O}_{39}\text{Mn}(\text{H}_2\text{O})]\}^{6+}$	3037	1635	993	948	903	798
$\text{K}_6[\text{SiW}_{11}\text{O}_{39}\text{Mn}(\text{H}_2\text{O})]$	—	—	998	957	903	809
$\{(\text{H}_4\mathbf{1})_2[\text{RuPOM}]\}^{7+}$	3052	1636	1003	956	910	785
Ru-POM^c	—	—	1006	960	913	777

^a ref. 1. ^b ref. 2. ^c ref. 4.

Table S3 Summary of redox potentials of the supramolecular assemblies of $\text{H}_4\mathbf{1}^{6+}$ (0.20 M) with POMs (0.10 M) in water (pH 3.0) containing NaCl (0.10 M) as an electrolyte at 297 K

	$E_{\text{red}2}^a$	$E_{\text{red}1}^a$	$E_{\text{ox}1}^a$
$\text{H}_4\mathbf{1}^{6+ b}$	—	-0.28	—
$\text{H}_4\mathbf{1}^{6+} + \text{K}_5\text{H}[\text{CoW}_{12}\text{O}_{40}]$	-0.98	-0.37	+0.71
$\text{K}_5\text{H}[\text{CoW}_{12}\text{O}_{40}]$	—	—	+0.81
$\text{H}_4\mathbf{1}^{6+} + \text{K}_7[\text{P}_2\text{W}_{17}\text{O}_{61}\text{Mn}(\text{H}_2\text{O})]$	-0.55	-0.32	+0.40
$\text{K}_7[\text{P}_2\text{W}_{17}\text{O}_{61}\text{Mn}(\text{H}_2\text{O})]$	—	—	+0.45
$\text{H}_4\mathbf{1}^{6+} + \text{Ru-POM}$	—	-0.40	+0.74
Ru-POM	—	—	+0.59

^a V vs. SCE. ^b pH 2.3.

Due to the low solubility of the supramolecular assemblies of $\text{H}_4\mathbf{1}^{6+}$ with POMs in water, clearly defined waves were not observed in the CVs, and thus, the redox potentials were determined with the peaks observed in the DPVs. As expected, the reduction potential ($E_{\text{red}1}$) of $\text{H}_4\mathbf{1}^{6+}$ was negatively shifted after formation of the supramolecular assemblies with negatively-charged POMs in common to the three POMs. On the other hand, the oxidation potentials ($E_{\text{ox}1}$) of the POMs did not show the common tendency after formation of the supramolecular assemblies, probably since the POMs exhibited different degree of interaction with the counter cations and protons in acidic water.

Table S4 Yields of 4-methylbenzaldehyde for the photocatalytic oxidation of MeBA and its control experiments under photoirradiation at 500 nm^a

Entry	RuPOM	H ₄ I ⁶⁺	Na ₂ S ₂ O ₈	<i>hν</i>	Yield, % ^b
1	Y	Y	Y	Y	18 (TON = 180)
2	N	Y	Y	Y	2
3	Y	N	Y	Y	2
4 ^c	Y	N	Y	Y	1
5	Y	Y	N	Y	0
6	Y	Y	Y	N	3
7	N	N	Y	N	0.5
8 ^d	N	N	Y	N	47
9	Y	N ^e	Y	Y	3

^a Reaction conditions: reaction time = 4 h, [RuPOM] = 2 μM, [H₄I⁶⁺] = 5 μM, [Na₂S₂O₈] = 2.2 mM, [4-methylbenzyl alcohol] = 2 mM. Light source: a Xe lamp (300 W, λ = 500 nm). Solvent: HCl aq (pD 3.0). Temperature: 298 K. ^b Yield = 100 × [Product]/[Substrate]₀. ^c Photoirradiation at 380 nm. ^d Temperature: 317 K. ^e Tetrakis(*N*-methyl-pyrid-4-yl)porphyrin chloride salt was used as the photosensitizer instead of H₄I⁶⁺.

Table S5 Dependence of yields of 4-methylbenzaldehyde for the photocatalytic oxidation of MeBA on the POM catalyst^a

Entry	POM	E_{ox} , V vs SCE	Yield, ^b %	TON
1	RuPOM	+0.59	18	180
2	$\text{K}_6[\text{GeW}_{11}\text{O}_{39}\text{Mn}(\text{H}_2\text{O})]$	+0.57	5	50
3	$\text{K}_7[\text{P}_2\text{W}_{17}\text{O}_{61}\text{Mn}(\text{H}_2\text{O})]$	+0.45	7	70
4	$\text{K}_4[\text{PW}_{11}\text{O}_{39}\text{Mn}(\text{H}_2\text{O})]$	+0.61	4	40
5	$\text{K}_5[\text{PW}_{11}\text{O}_{39}\text{Mn}(\text{H}_2\text{O})]$	+0.62	12	120
6	$\text{K}_6[\text{SiW}_{11}\text{O}_{39}\text{Mn}(\text{H}_2\text{O})]$	+0.45	3	30

^a Reaction conditions: reaction time = 4 h, [POM] = 2 μM , [$\text{H}_4\mathbf{1}^{6+}$] = 5 μM , [$\text{Na}_2\text{S}_2\text{O}_8$] = 2.2 mM, [4-methylbenzyl alcohol] = 2 mM. Light source: a Xe lamp (300 W, λ = 500 nm). Solvent: HCl aq (pD 3.0). Temperature: 298 K. ^b Yield = $100 \times [\text{Product}]/[\text{Substrate}]_0$.

Among the five kinds of MnPOMs used here, $\text{K}_5[\text{PW}_{11}\text{O}_{39}\text{Mn}(\text{H}_2\text{O})]$ afforded the highest product yield and TON (entry 5), which was still lower than that of RuPOM (entry 1). $\text{K}_5[\text{PW}_{11}\text{O}_{39}\text{Mn}(\text{H}_2\text{O})]$ has a very similar structure and oxidation potential to those of RuPOM, which possibly explains its relatively higher catalytic activity.

Table S6 Crystallographic data for [H₄1⁶⁺]Cl₆

Crystal system	Monoclinic
Space group	<i>C2/c</i>
<i>T</i> , K	120
Formula	C ₁₁₆ H ₈₈ N ₈ Cl ₆
Formula weight	1806.74
<i>a</i> , Å	43.317(9)
<i>b</i> , Å	23.984(4)
<i>c</i> , Å	29.932(7)
α , °	90
β , °	117.762(4)
γ , °	90
<i>V</i> , Å ³	26597.9
<i>Z</i>	8
λ (Mo K α), Å	0.71073
<i>D</i> _c , g cm ⁻³	0.902
Reflections measured	75266
Reflections unique	30916
<i>R</i> 1 (<i>I</i> > 2 σ (<i>I</i>))	0.111
<i>wR</i> 2 (all)	0.322
GOF	1.077